Phillips MJ, Page TJ, de Bruyn M, Huey JA, Humphreys WF, Hughes JM, Santos SR, Schmidt DJ, Waters JM (2013) The linking of plate tectonics and evolutionary divergence. *Current Biology*, 23, R603-R605.

Whereas cohesin cleavage alone did not produce any detectable effects on engaged centrioles, Cdk inhibition, in contrast, was sufficient to induce centriole disengagement even in the absence of proper chromosome disjunction. Upon p27 injection, centriole disengagement was observed with a similar kinetics to the disengagement observed in the TEV+p27 experiments (Figure 1).

Our previous experiments revealed that Cdk inactivation in metaphase-arrested embryos was not accompanied by prompt separase activation, as sister chromatids did not move apart during induced mitotic exit [6]. Our results therefore also raise the possibility that separase is not universally involved in centriole disengagement. In agreement, previous studies in *Drosophila* failed to detect any centrosome duplication defects in separase mutant embryos [8].

While Cdk inhibition was sufficient to trigger centriole disengagement, no further separation of sister centrioles could be observed. This finding suggests that even in *Drosophila* embryos, where centriole disengagement is immediately followed by centrosome separation, these are mechanistically different processes: centriole disengagement appears to depend on a drop in Cyclin-B–Cdk activity whereas centrosome separation is likely to depend on a subsequent rise of cyclin B levels and/or DNA replication.

In summary, in contrast to the recent observation in mammalian cells, our experiments support the idea that centriole engagement does not depend on the integrity of the cohesin complex, at least in *Drosophila* embryos. In agreement, recent studies propose that cleavage of a novel centrosomal substrate for separase — pericentrin/kendrin — is required for centriole disengagement [9]. Importantly, our experiments further demonstrate that centriole disengagement during mitotic exit, as many other aspects of this key transition, can be negatively regulated by Cdk activity. This supports a role for Cdk1 in preventing premature centriole disengagement in *Drosophila* early embryos. Further experiments will be required to investigate whether this results from a direct Cdk-dependent phosphorylation of centrosome components or rather an indirect consequence of changing pericentriolar organization or microtubule forces, as recently suggested [10].

Supplemental Information

Supplemental Information includes one figure and experimental procedures and can be found with this article online at http://dx.doi.org/10.1016/j.cub.2013.04.003.

Acknowledgments

We would like to acknowledge Jean Metson for technical assistance. We thank Alexander Dammermann for sharing unpublished data, Jordan Raff and Monica Bettencourt-Dias for advice and comments on the manuscript, Jordan Raff for the Sas4 cDNA and Micron Oxford for excellent help with microscopy. Work in the laboratory of K.N. is supported by grants from Medical Research Council (MRC), the Wellcome Trust and the European Research Council (ERC).

References

1. Tsou, M.F., and Stearns, T. (2006). Mechanism limiting centrosome duplication to once per cell cycle. Nature *442*, 947–951.
2. Tsou, M.F., Wang, W.J., George, K.A., Uryu, K., Stearns, T., and Jallepalli, P.V. (2009). Polo kinase and separase regulate the mitotic licensing of centriole duplication in human cells. Dev. Cell *17*, 344–354.
3. Schockel, L., Mockel, M., Mayer, B., Boos, D., and Stemmann, O. (2011). Cleavage of cohesin rings coordinates the separation of centrioles and chromatids. Nat. Cell Biol. *13*, 966–972.
4. Oliveira, R.A., and Nasmyth, K. (2010). Getting through anaphase: splitting the sisters and beyond. Biochem. Soc. Trans. *38*, 1639–1644.
5. Simmons Kovacs, L.A., and Haase, S.B. (2010). Cohesin: it's not just for chromosomes anymore. Cell Cycle *9*, 1750–1753.
6. Oliveira, R.A., Hamilton, R.S., Pauli, A., Davis, I., and Nasmyth, K. (2010). Cohesin cleavage and Cdk inhibition trigger formation of daughter nuclei. Nat. Cell Biol. *12*, 185–192.
7. Pauli, A., Althoff, F., Oliveira, R.A., Heidmann, S., Schuldiner, O., Lehner, C.F., Dickson, B.J., and Nasmyth, K. (2008). Cell-type-specific TEV protease cleavage reveals cohesin functions in Drosophila neurons. Dev. Cell *14*, 239–251.
8. Pandey, R., Heidmann, S., and Lehner, C.F. (2005). Epithelial re-organization and dynamics of progression through mitosis in Drosophila separase complex mutants. J. Cell Sci. *118*, 733–742.
9. Matsuo, K., Ohsumi, K., Iwabuchi, M., Kawamata, T., Ono, Y., and Takahashi, M. (2012). Kendrin is a novel substrate for separase involved in the licensing of centriole duplication. Curr. Biol. *22*, 915–921.
10. Cabral, G., Sanegre Sans, S., Cowan, C.R., and Dammermann, A. (2013). Multiple mechanisms contribute to centriole separation in *C. elegans*. Curr. Biol. *23*, 1380–1387.

[1]Instituto Gulbenkian de Ciência, Rua da Quinta Grande, 6, 2780–156 Oeiras, Portugal. [2]Department of Biochemistry, University of Oxford, South Parks Road, Oxford, OX1 3QU, UK.
*E-mail: rcoliveira@igc.gulbenkian.pt

The linking of plate tectonics and evolutionary divergence

Matthew J. Phillips[1,*,§], Timothy J. Page[2§], Mark de Bruyn[3], Joel A. Huey[2], William F. Humphreys[4], Jane M. Hughes[2], Scott R. Santos[5], Daniel J. Schmidt[2], and Jonathan M. Waters[6]

It is exciting to be living at a time when the big questions in biology can be investigated using modern genetics and computing [1]. Bauzà-Ribot *et al.* [2] take on one of the fundamental drivers of biodiversity, the effect of continental drift in the formation of the world's biota [3,4], employing next-generation sequencing of whole mitochondrial genomes and modern Bayesian relaxed molecular clock analysis. Bauzà-Ribot *et al.* [2] conclude that vicariance via plate tectonics best explains the genetic divergence between subterranean metacrangonyctid amphipods currently found on islands separated by the Atlantic Ocean. This finding is a big deal in biogeography, and science generally [3], as many other presumed biotic tectonic divergences have been explained as probably due to more recent transoceanic dispersal events [4]. However, molecular clocks can be problematic [5,6] and we have identified three issues with the analyses of Bauzà-Ribot *et al.* [2] that cast serious doubt on their results and conclusions. When we reanalyzed their mitochondrial data and attempted to account for problems with calibration [5,6], modeling rates across branches [5,7] and substitution saturation [5], we inferred a much younger date for their key node. This implies either a later trans-Atlantic dispersal of these crustaceans, or more likely a series of later invasions of freshwaters from a common marine ancestor, but either way probably not ancient tectonic plate movements.

Bauzà-Ribot *et al.* [2] use up-to-date molecular dating methods, with calibrations from two paleogeographic events derived from presumed vicariant splits (in the Moroccan High-Atlas 37.2–25.0 mya (million years ago) and the Mediterranean 16–5.5 mya). Because rates of molecular evolution can vary greatly between lineages

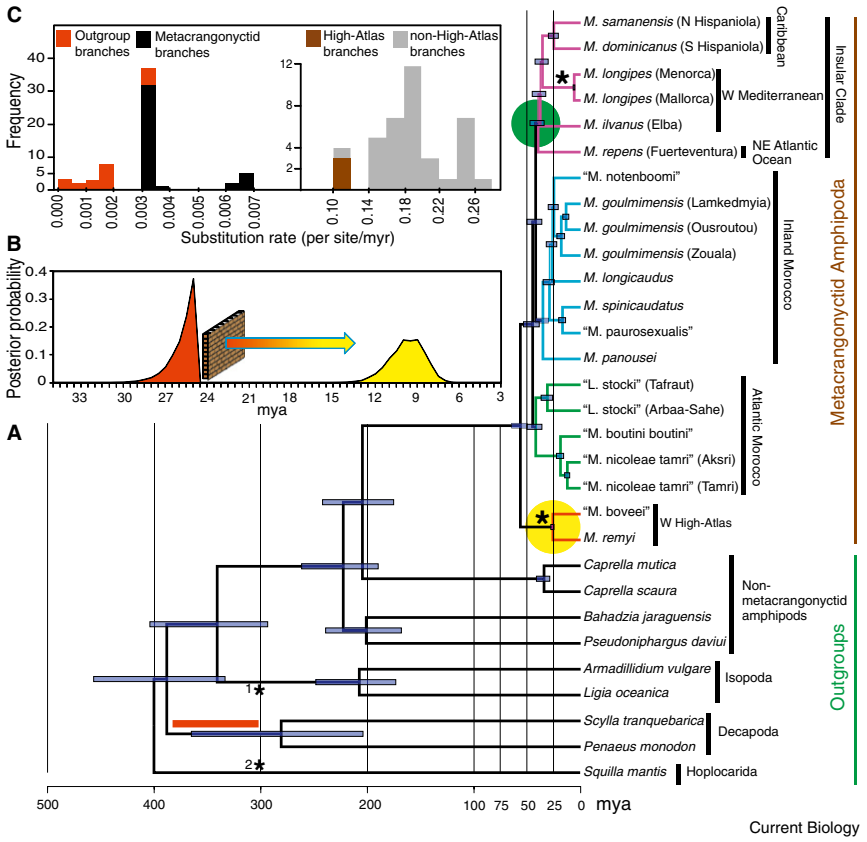

Figure 1. Revised time frame for metacrangonyctid diversification.
(A) BEAST random local clock timetree employing paleogeographic calibration bounds (asterisks represent calibrations) and fossil calibration at the root, with the 95% soft bounds prior indicated by a red bar and the associated minimum bound fossils indicated (asterisk 1 for the isopod, *Hesslerella* and asterisk 2 for the hoplocarid, *Gorgonophontes*). Blue bars are 95% highest posterior distributions (HPDs). Green circle highlights divergence of Trans-Atlantic clades and dates to 39.9 mya (47.5–34.3 mya 95% HPD). Yellow circle highlights the High-Atlas calibration node. (B) Posterior age distributions for the highlighted High-Atlas calibration node when both fossil and paleogeographic calibrations are used (red on left) with a 'hard' lower boundary (i.e. brick wall at 25 mya); and when only fossil calibration is used (in yellow on right). (C) Posterior distributions of substitution rates along branches, inferred under random local clocks for the full taxon set (third codon positions excluded; left side) and for metacrangonyctids alone (all codon positions; right side). Root calibrations only were employed for inferring these distributions, thus avoiding rate distortion owing to conflict between calibrations (Supplemental information).

and over time, multiple calibrations in different parts of the tree may reduce this error [5], though they are no panacea [6]. We have several concerns with their dating inference. First, they estimate deep node ages from far younger calibrated nodes, without also placing bounds deeper in the tree. This kind of extrapolation can multiply rate-errors for deep nodes and led Thorne and Kishino [8] to require a root prior, such that dates are instead interpolated between calibrations. Bauzà-Ribot *et al*.'s [2] High-Atlas calibration largely drives the divergence estimates, which in their various analyses closely converged with or without the Mediterranean calibration. However, the lack of non-metacrangonyctid outgroups in their molecular clock analyses may preclude accurate rate estimation across the root (between the High-Atlas calibration and the trans-Atlantic clade). A similar problem caused a two-fold age overestimation in monotremes [9]. To address this concern, we have added various outgroups (amphipods and deeper-diverging malacostracans) which allowed us to place a fossil calibration prior on the root of the tree (Supplemental information) while also retaining the younger biogeographic calibrations from Bauzà-Ribot *et al*. [2].

Second, we note that the mitochondrial third codon positions are highly saturated, averaging more than eight superimposed substitutions per site along some ingroup branches and far more among outgroup branches. Bauzà-Ribot *et al*. [2] test only for saturation extinguishing phylogenetic signal and not its impact on branch length estimation, which is directly relevant to molecular dating. We show that available substitution models under-correct for third codon position saturation in Bauzà-Ribot *et al*.'s [2] original dataset by ~15% (Supplemental information), so third codon positions were excluded in our analyses. A third concern that is exacerbated by the need to include outgroups is that the distribution of rates across the tree is not lognormally distributed (Supplemental information), as assumed in Bauzà-Ribot *et al*.'s [2] analyses by their choice of model. Rates among their metacrangonyctids are distributed at least bimodally, with outgroups adding an additional rate region (Figure 1C). Instead of the lognormal distribution model, we use the more flexible random local clocks model [10], but otherwise maintain the same substitution models and tree priors to reanalyze the data.

Our result for the divergence linking both sides of the Atlantic was 39.9 mya (47.5–34.3 mya 95% highest posterior distribution, HPD; Figure 1A). The posterior distributions for the two biogeographic calibrations strongly conflict with the fossil calibration, are tightly pressed to their minima when enforced and fall much younger when free (Figure 1B), implying these events may not be associated with the chosen divergences. Upon excluding the two biogeographic calibrations, the trans-Atlantic divergence becomes even more recent at 20.3 mya (24.9–15.8 mya 95% HPD; Supplemental information).

Bauzà-Ribot *et al*. [2] lay out a clear biogeographic hypothesis that the widening and deepening of the Tethys Sea around 110–95 mya explains the trans-Atlantic divergence, and adopt this vicariant conclusion based on their 79 mya (108–60 mya 95% HPD) dating of the trans-Atlantic divergence. Bauzà-Ribot *et al*. [2] suggest that younger inferred divergence times would lend credence to a dispersal scenario from the old world to the new, which fits with our results better. This should come as no surprise, as Bauzà-Ribot *et al*. [2] say that the ancestral population of these freshwater taxa was a wide-ranging marine species ('thalassoid'), and therefore must have independently colonized caves in each location later (as is common in subterranean

fauna [3]). Some might suggest that the island home of every member of the relevant trans-Atlantic clade (Hispaniola, Fuerteventura, Mallorca, Menorca, Elba) would actually imply that this lineage was an active and successful disperser at times, instead of being only a passive passenger on tectonic plates.

Rather than providing a definitive answer, our results and conclusions highlight the difficult nature of some of biology's big questions. Given the rapid substitution rates (in both our and Bauzà-Ribot *et al*. [2] analyses) and the great age of the question being considered, slower evolving nuclear sequences [1] may be better suited to this particular biogeographic question.

Supplemental Information

Supplemental Information including supplemental results, methods and one figure can be found with this article online at http://dx.doi.org/10.1016/j.cub.2013.06.001.

References

1. Emerson, B.C., and Hewitt, G.M. (2005). Phylogeography. Curr. Biol. *15*, R367–R371.
2. Bauzà-Ribot, Maria M., Juan, C., Nardi, F., Oromí, P., Pons, J., and Jaume, D. (2012). Mitogenomic phylogenetic analysis supports continental-scale vicariance in subterranean thalassoid crustaceans. Curr. Biol. *22*, 2069–2074.
3. Maderspacher, F. (2012). Evolution: drift will tear us apart. Curr. Biol. *22*, R909–R912.
4. Crisp, M.D., Trewick, S.A., and Cook, L.G. (2011). Hypothesis testing in biogeography. Trends Ecol. Evol. *26*, 66–72.
5. Pulquério, M.J.F., and Nichols, R.A. (2007). Dates from the molecular clocks: how wrong can we be? Trends Ecol. Evol. *22*, 180–184.
6. Heads, M. (2012). Bayesian transmogrification of clade divergence dates: a critique. J. Biogeogr. *39*, 1749–1756.
7. Phillips, M.J. (2009). Branch-length estimation bias misleads molecular dating for a vertebrate mitochondrial phylogeny. Gene *441*, 132–140.
8. Thorne, J.L., and Kishino, H. (2002). Divergence time and evolutionary rate estimation with multilocus data. Syst. Biol. *51*, 689–702.
9. Phillips, M.J., Bennett, T., and Lee, M.S. (2009). Molecules, morphology, and ecology indicate a recent, amphibious ancestry for echidnas. Proc. Nat. Acad. Sci. U.S.A. *106*, 17089–17094.
10. Drummond, A.J., and Suchard, M.A. (2010). Bayesian random local clocks, or one rate to rule them all. BMC Biol. *8*, 114.

[1]School of Earth, Environmental and Biological Sciences, Queensland University of Technology, Brisbane, QLD, 4001, Australia. [2]Australian Rivers Institute, Griffith University, Nathan, QLD, 4111, Australia. [3]Molecular Ecology & Fisheries Genetics Laboratory, School of Biological Sciences, Bangor University, Bangor, LL57 2UW, UK. [4]Western Australian Museum, Locked Bag 49, Welshpool DC, WA, 6986, Australia. [5]Department of Biological Sciences, Auburn University, Auburn, AL 36849, USA. [6]Department of Zoology, University of Otago, PO Box 56, Dunedin, 9054, New Zealand. §These authors contributed equally.
*E-mail: m9.phillips@qut.edu.au

Reply to Phillips *et al.*

Maria M. Bauzà-Ribot[1], Carlos Juan[1], Francesco Nardi[2], Pedro Oromí[3], Joan Pons[4*] and Damià Jaume[4]

Phillips *et al.* [1] reply to our finding that genetic divergence between subterranean metacrangonyctid amphipods from opposite shores of the Atlantic is congruent with vicariance by plate tectonics [2]. They highlight three presumed shortcomings in our analyses: first, the third codon positions of the mitochondrial genes used to reconstruct the metacrangonyctid phylogeny are saturated and consequently should be excluded from the analysis; second, substitution rates across the tree do not fit an uncorrelated lognormally distributed (UCLD) clock, and implementation of a random local clock (RLC) model would be more appropriate; third, the two dates that we used to calibrate the tree are fairly recent compared to the overall tree length, while the inclusion of a deep fossil calibrator could have improved dating. However, much of the criticism of Phillips *et al.* applies more to their modification of our data set than to the original data themselves. Specifically, their addition of several highly divergent taxa — driven by the necessity to include taxa encompassing the new deep calibration node they propose — largely alters the properties of our original data matrix. We maintain that third codon position saturation and deviation from lognormal rates largely apply to the new and not to the original data set. We also have some concerns about the fossil calibration used by Phillips *et al.* [1].

Both the stemminess metric calculated by Phillips *et al.* [1] and our Xia and Lemey test indicate that third codon positions are indeed more saturated than first and second positions. However, values for each of the three codon positions in our original dataset are lower than critical values [2], suggesting that there is still phylogenetic signal at third positions despite partial saturation. That third mitochondrial codon positions are partially saturated is no surprise and has been extensively demonstrated at various taxonomic levels [3]. However, the occurrence of partial saturation does not necessarily imply lack of phylogenetic signal and implementation of partitioning over codon positions and relaxed-clock models has been shown to improve molecular phylogenetic and dating analyses in such circumstances [4]. Notwithstanding, in order to evaluate the relevance of this argument analytically, we reanalyzed our data after exclusion of third codon positions and we show that this modification has a limited impact on age estimates (mean age 9% younger for node of the Atlantic clade) (Figure 1; Supplemental information).

Phillips *et al*. [1] also point out that rates are not lognormally distributed across our tree, although this seems to be mainly caused by the addition of distant outgroups [1]. In order to explicitly compare the two clock models (UCLD and RLC) in a formal phylogenetic Bayesian framework, we used the posterior simulation-based analog of Akaike's information criterion recently developed by Baele *et al*. [5]. The test indicates that UCLD clock, implemented in the original analysis, outperforms RLC (Supplemental information). For the sake of comparison, we nevertheless reanalyzed the original dataset, with and without third codon positions, applying a RLC model as suggested by [1]. New age estimates, although generally younger, still fall within the confidence age interval estimated using UCLD clocks (Figure 1), indicating that the original results are robust with respect to the use of different clock models and the effect of third codon positions.

Phillips *et al.* also refer to clock calibration issues [1]. We fully agree that, ideally, molecular clock calibrations are best implemented by deploying several well-dated fossils robustly assigned to particular nodes positioned at different timescales in a given phylogeny [3]. However, fossil calibrations in molecular phylogenies are far from being a silver bullet, for several reasons: fossils may be incorrectly assigned to the crown and not to the stem of a clade; fossils may be considerably younger than the origin of their respective clade; and data limitations may compromise both fossil taxonomic placement and dating [3,6]. Furthermore, the fossil record is notoriously incomplete, and in many instances appropriate

fauna [3]). Some might suggest that the island home of every member of the relevant trans-Atlantic clade (Hispaniola, Fuerteventura, Mallorca, Menorca, Elba) would actually imply that this lineage was an active and successful disperser at times, instead of being only a passive passenger on tectonic plates.

Rather than providing a definitive answer, our results and conclusions highlight the difficult nature of some of biology's big questions. Given the rapid substitution rates (in both our and Bauzà-Ribot *et al*. [2] analyses) and the great age of the question being considered, slower evolving nuclear sequences [1] may be better suited to this particular biogeographic question.

Supplemental Information

Supplemental Information including supplemental results, methods and one figure can be found with this article online at http://dx.doi.org/10.1016/j.cub.2013.06.001.

References

1. Emerson, B.C., and Hewitt, G.M. (2005). Phylogeography. Curr. Biol. *15*, R367–R371.
2. Bauzà-Ribot, Maria M., Juan, C., Nardi, F., Oromí, P., Pons, J., and Jaume, D. (2012). Mitogenomic phylogenetic analysis supports continental-scale vicariance in subterranean thalassoid crustaceans. Curr. Biol. *22*, 2069–2074.
3. Maderspacher, F. (2012). Evolution: drift will tear us apart. Curr. Biol. *22*, R909–R912.
4. Crisp, M.D., Trewick, S.A., and Cook, L.G. (2011). Hypothesis testing in biogeography. Trends Ecol. Evol. *26*, 66–72.
5. Pulquério, M.J.F., and Nichols, R.A. (2007). Dates from the molecular clocks: how wrong can we be? Trends Ecol. Evol. *22*, 180–184.
6. Heads, M. (2012). Bayesian transmogrification of clade divergence dates: a critique. J. Biogeogr. *39*, 1749–1756.
7. Phillips, M.J. (2009). Branch-length estimation bias misleads molecular dating for a vertebrate mitochondrial phylogeny. Gene *441*, 132–140.
8. Thorne, J.L., and Kishino, H. (2002). Divergence time and evolutionary rate estimation with multilocus data. Syst. Biol. *51*, 689–702.
9. Phillips, M.J., Bennett, T., and Lee, M.S. (2009). Molecules, morphology, and ecology indicate a recent, amphibious ancestry for echidnas. Proc. Nat. Acad. Sci. U.S.A. *106*, 17089–17094.
10. Drummond, A.J., and Suchard, M.A. (2010). Bayesian random local clocks, or one rate to rule them all. BMC Biol. *8*, 114.

[1]School of Earth, Environmental and Biological Sciences, Queensland University of Technology, Brisbane, QLD, 4001, Australia. [2]Australian Rivers Institute, Griffith University, Nathan, QLD, 4111, Australia. [3]Molecular Ecology & Fisheries Genetics Laboratory, School of Biological Sciences, Bangor University, Bangor, LL57 2UW, UK. [4]Western Australian Museum, Locked Bag 49, Welshpool DC, WA, 6986, Australia. [5]Department of Biological Sciences, Auburn University, Auburn, AL 36849, USA. [6]Department of Zoology, University of Otago, PO Box 56, Dunedin, 9054, New Zealand. §These authors contributed equally.
*E-mail: m9.phillips@qut.edu.au

Reply to Phillips *et al.*

Maria M. Bauzà-Ribot[1], Carlos Juan[1], Francesco Nardi[2], Pedro Oromí[3], Joan Pons[4*] and Damià Jaume[4]

Phillips *et al.* [1] reply to our finding that genetic divergence between subterranean metacrangonyctid amphipods from opposite shores of the Atlantic is congruent with vicariance by plate tectonics [2]. They highlight three presumed shortcomings in our analyses: first, the third codon positions of the mitochondrial genes used to reconstruct the metacrangonyctid phylogeny are saturated and consequently should be excluded from the analysis; second, substitution rates across the tree do not fit an uncorrelated lognormally distributed (UCLD) clock, and implementation of a random local clock (RLC) model would be more appropriate; third, the two dates that we used to calibrate the tree are fairly recent compared to the overall tree length, while the inclusion of a deep fossil calibrator could have improved dating. However, much of the criticism of Phillips *et al.* applies more to their modification of our data set than to the original data themselves. Specifically, their addition of several highly divergent taxa — driven by the necessity to include taxa encompassing the new deep calibration node they propose — largely alters the properties of our original data matrix. We maintain that third codon position saturation and deviation from lognormal rates largely apply to the new and not to the original data set. We also have some concerns about the fossil calibration used by Phillips *et al.* [1].

Both the stemminess metric calculated by Phillips *et al.* [1] and our Xia and Lemey test indicate that third codon positions are indeed more saturated than first and second positions. However, values for each of the three codon positions in our original dataset are lower than critical values [2], suggesting that there is still phylogenetic signal at third positions despite partial saturation. That third mitochondrial codon positions are partially saturated is no surprise and has been extensively demonstrated at various taxonomic levels [3]. However, the occurrence of partial saturation does not necessarily imply lack of phylogenetic signal and implementation of partitioning over codon positions and relaxed-clock models has been shown to improve molecular phylogenetic and dating analyses in such circumstances [4]. Notwithstanding, in order to evaluate the relevance of this argument analytically, we reanalyzed our data after exclusion of third codon positions and we show that this modification has a limited impact on age estimates (mean age 9% younger for node of the Atlantic clade) (Figure 1; Supplemental information).

Phillips *et al*. [1] also point out that rates are not lognormally distributed across our tree, although this seems to be mainly caused by the addition of distant outgroups [1]. In order to explicitly compare the two clock models (UCLD and RLC) in a formal phylogenetic Bayesian framework, we used the posterior simulation-based analog of Akaike's information criterion recently developed by Baele *et al*. [5]. The test indicates that UCLD clock, implemented in the original analysis, outperforms RLC (Supplemental information). For the sake of comparison, we nevertheless reanalyzed the original dataset, with and without third codon positions, applying a RLC model as suggested by [1]. New age estimates, although generally younger, still fall within the confidence age interval estimated using UCLD clocks (Figure 1), indicating that the original results are robust with respect to the use of different clock models and the effect of third codon positions.

Phillips *et al.* also refer to clock calibration issues [1]. We fully agree that, ideally, molecular clock calibrations are best implemented by deploying several well-dated fossils robustly assigned to particular nodes positioned at different timescales in a given phylogeny [3]. However, fossil calibrations in molecular phylogenies are far from being a silver bullet, for several reasons: fossils may be incorrectly assigned to the crown and not to the stem of a clade; fossils may be considerably younger than the origin of their respective clade; and data limitations may compromise both fossil taxonomic placement and dating [3,6]. Furthermore, the fossil record is notoriously incomplete, and in many instances appropriate

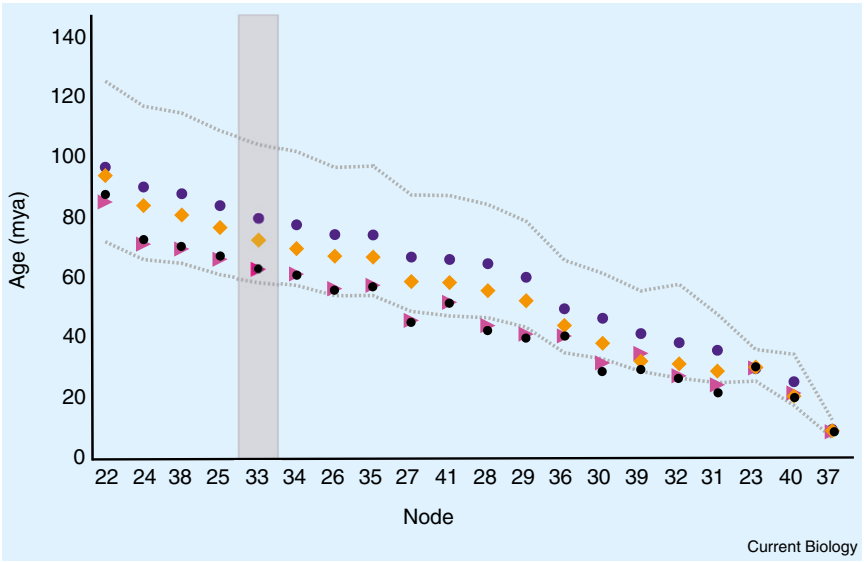

Figure 1. Estimation of node ages under relaxed lognormal and random local clocks.
Comparison of node age estimates obtained using different analyses. Common to all are the palaeogeographical events used for calibration, the phylogenetic tree and corresponding node numbers reported in [2] and the use of independent substitution models and clocks for each codon site. Original analysis (uncorrelated lognormal relaxed clock, third codon positions included): blue dots represent mean estimates, gray lines represent 95% HPD intervals. Data reanalysis: orange squares represent mean estimates applying an uncorrelated lognormal clock model with third codon positions excluded; pink triangles with random local clocks and third codon positions included, black dots with random local clocks and third codon positions excluded. The key node linking both sides of the Atlantic in the phylogeny reported in [2] is highlighted with a grey box.

fossil calibrators are simply not available. In fact, the fossil record of the Amphipoda is extremely poor, with the oldest fossils known corresponding to casts preserved in Eocene Baltic amber no older than 54–40 million years (my) [7] (Supplemental information). Without an appropriate fossil calibrator for the taxa under investigation, Phillips *et al.* [1] add a number of non-metacrangonyctid amphipod, isopod, decapod and hoplocarid outgroups to our original alignment [1], in order to encompass an inferred date for the separation of the Subclasses Eumalacostraca and Hoplocarida derived from fossil information. In doing so, they introduce two possible problems. This is an extremely deep node in relation to our ingroup, and raises significant concern over the overall rate stability. Furthermore, they used the age of *Hesslerella* to date the split of the Subclasses Eumalacostraca and Hoplocarida, seemingly overlooking that *Hesslerella* is an undeniable crown-group phreatoicidean [8,9], a member of the Peracarid order Isopoda, and as such its age (325 mya) should be considered a *minimum* constraint age for the Peracarida. Thus, it should be assigned to the node Isopoda/Amphipoda in Phillips *et al.*'s [1] tree instead of to the Hoplocarida/Eumalacostraca node. It is important to mention here that the Eumalacostraca includes three Superorders: Syncarida, Eucarida (to which the decapods belong) and Peracarida, the latter including the amphipods and Isopods, among other groups (Supplemental information).

The calibration of molecular clocks and deduction of subsequent evolutionary timescales have always been open to debate and discussion [3,6]. We acknowledge that there are a number of assumptions and parameters that can be applied to both phylogeny estimation and molecular clock calibration that can have an impact on the resulting estimates. A full understanding of the relative importance of vicariance and dispersal to explain the distribution of metacrangonyctid amphipods would require taxonomically well-sampled, robust multi-loci phylogenies of the lineages forming the superorder Peracarida, with reliable and appropriately distributed palaeographic and fossil calibrations.

The criticisms of Philips *et al.* [1] demonstrate the power of parameter choice to drive biogeographic inference. Their differing results are largely driven by the modification of the original dataset and a possibly inappropriate deployment of fossil calibration. Potentially powerful parameters do indeed carry great responsibility.

Supplemental Information

Supplemental Information including additional discussion and one figure can be found with this article online at http://dx.doi.org/10.1016/j.cub.2013.04.017.

Acknowledgments

We acknowledge the help and suggestions of Brent Emerson and José Castresana. This work was supported by Spanish grants CGL2009-08256, CGL2012-33597 and CSIC Intramural grant 200930I141.

References

1. Phillips, M.J., Page, T.J., de Bruyn, M., Huey, J.A., Humphreys, W.F., Hughes, J.M., Santos, S.R., Schmidt, D.J., and Waters, J.M. (2013). The linking of plate tectonics and evolutionary divergences. Curr. Biol. *23*, R603–R605.
2. Bauzà -Ribot, M.M., Juan, C., Nardi, F., Oromí, P., Pons, J., and Jaume, D. (2012). Mitogenomic phylogenetic analysis supports continental-scale vicariance in subterranean thalassoid crustaceans. Curr. Biol. *22*, 2069–2074.
3. Lukoschek, V., Keogh, J.S, and Avise, J.C. (2012). Evaluating fossil calibrations for dating phylogenies in light of rates of molecular evolution: a comparison of three approaches. Systemat. Biol. *61*, 22–43.
4. Ho, S.Y.W., and Lanfear, R. (2010). Improved characterisation of among-lineage rate variation in cetacean mitogenomes using codon-partitioned relaxed clocks. Mitochondrial DNA *21*, 138–146.
5. Baele, G., Li WLS, Drummond, A.J., Suchard, M.A., and Lemey, P. (2012). Accurate model selection of relaxed molecular clocks in Bayesian phylogenetics. Mol. Biol. Evol. *30*, 239–243.
6. Donoghue, P.C.J., and Benton, M.J. (2007). Rocks and clocks: calibrating the tree of life using fossils and molecules. Trends Ecol. and Evol. *22*, 424–431.
7. Coleman, C.O. (2006). An amphipod of the genus Synurella Wrzesniowski, 1877 (Crustacea, Amphipoda, Crangonyctidae) found in Baltic amber. Organisms Diversity Evol. *6*, 103–108.
8. Schram, F.R. (1974). Paleozoic Peracarida of North America. Fieldiana Geol. *33*, 95–124.
9. Wilson, G.D.F., and Edgecombe G. (2003). The Triassic isopod Protamphisopus wianamattensis (Chilton) and comparison with extant taxa (Crustacea, Phreatoicidea). J. Paleontol. *77*, 454–470.

[1]Departament de Biologia, Universitat de les Illes Balears, 07122 Palma, Spain. [2]Department of Life Sciences, University of Siena, via Aldo Moro 2, 53100 Siena, Italy. [3]Departmento de Biología Animal, Universidad La Laguna, 38205 La Laguna, Tenerife, Canary Islands, Spain. [4]IMEDEA (CSIC-UIB), Mediterranean Institute for Advanced Studies, c/ Miquel Marquès 21, 07190 Esporles, Spain.
*E-mail: jpons@imedea.uib-csic.es

Current Biology 22, 2069–2074, November 6, 2012 ©2012 Elsevier Ltd All rights reserved http://dx.doi.org/10.1016/j.cub.2012.09.012

Report

Mitogenomic Phylogenetic Analysis Supports Continental-Scale Vicariance in Subterranean Thalassoid Crustaceans

Maria M. Bauzà-Ribot,[1] Carlos Juan,[1] Francesco Nardi,[2] Pedro Oromí,[3] Joan Pons,[4,*] and Damià Jaume[4]
[1]Departament de Biologia, Universitat de les Illes Balears, 07122 Palma, Spain
[2]Department of Evolutionary Biology, University of Siena, via Aldo Moro 2, 53100 Siena, Italy
[3]Departmento de Biología Animal, Universidad La Laguna, 38205 La Laguna, Tenerife, Canary Islands, Spain
[4]IMEDEA (CSIC-UIB), Mediterranean Institute for Advanced Studies, c/ Miquel Marquès 21, 07190 Esporles, Spain

Summary

Many continental subterranean water crustaceans ("stygobionts") display extreme disjunct distributions, where different species in the same genus are isolated on continents or islands separated by broad oceanic expanses [1]. Despite their freshwater habitat, most of these taxa appear to be most closely related to typical marine groups ("thalassoid" origin) [2]. Among the hadzioids—thalassoid amphipods including the stygobiont families Hadziidae, Pseudoniphargidae, and Metacrangonyctidae—several genera are restricted to inland groundwaters ranging from the Caribbean region to the Mediterranean and Middle East, including interspersed oceanic islands [3]. This distribution might have arisen from Tethyan vicariance [4–7] triggered by the sequential occlusion of the former Tethys Sea, a vast circumtropical ocean existing from the Middle Jurassic up to 20 million years ago (mya). Previous studies have been based on morphological analyses or limited DNA sequence data, making it difficult to test this hypothesis [8–10]. We used complete mitochondrial protein-coding gene sequences, mainly obtained by next-generation sequencing methods and a nuclear ribosomal gene to resolve the phylogeny and to establish a time frame for diversification of the family Metacrangonyctidae (Amphipoda). The results were consistent with the plate tectonics vicariance hypothesis, with major diversifications occurring between 96 and 83 mya.

Results and Discussion

For many years, a key question in zoogeography has been the origin of the extremely disjunct distribution patterns of stygobiont crustaceans after the discovery of Caribbean lineages related to Mediterranean taxa [1]. This distribution pattern exhibited by many genera of thalassoid stygobiont crustaceans is currently explained as a vicariant process whereby plate tectonics caused the fragmentation of a marine ancestor's range, once continuously distributed along the shores of ancient seas [4–6]. This might have been followed by secondary isolation and subsequent speciation in brackish or limnic groundwaters, a process triggered by episodes of sea-level oscillation or of tectonic uplift at coastal areas [5, 7]. Other alternative hypotheses, such as broad-range, open-water marine dispersal are also possible for crustaceans with free-swimming larval stages [1, 11]. In addition, deep-sea dispersal along the crevicular medium associated with the circumglobal system of spreading zones has also been suggested to explain the presence of some of these taxa in geologically young oceanic islands [8, 12].

Testing among these alternative hypotheses requires robust phylogenies and accurate calibration points to derive a reliable estimation of divergence times [8, 9]. Transoceanic dispersal cannot be discarded a priori in stygobiont groups exhibiting a presumed Tethyan distribution but with shallow genetic divergences. Thus, to lend credence to the ancient vicariant origin hypothesis, divergence times between phylogenetic sister lineages placed at opposite sides of the Atlantic should be older than the establishment of deep-water conditions between Iberia and North America at about 95–110 million years ago (mya) [13, 14].

Here we studied the phylogeny of the Metacrangonyctidae, a family of stygobiont amphipod crustaceans with representatives in Hispaniola (Antilles), the Canary Islands, and around the Mediterranean region and the Middle East [15] (Figure 1). This monophyletic taxon [16] comprises two genera, *Metacrangonyx* Chevreux, 1909 and *Longipodacrangonyx* Boutin and Messouli, 1988, including a total of 18 species formally described—11 of which are limited to Morocco—plus at least 18 additional Moroccan taxa still awaiting formal description [16, 17]. The presence of two species of *Metacrangonyx* in the Caribbean region [18] offers an unmatched opportunity to test through phylogenetic analyses the role of dispersal and vicariance in the establishment of disjunct transoceanic distribution patterns in stygobiont crustaceans. We have sequenced the complete mitochondrial genome (~16 kb) (mitogenome) and the nuclear *SSU* ribosomal gene of 21 divergent lineages within 16 metacrangonyctid species and two outgroup taxa (Table 1; see Supplemental Experimental Procedures available online). The data set includes the recently characterized mitogenome of *Metacrangonyx longipes* Chevreux, 1909, from Mallorca (Balearic Islands) [19]. Species were chosen to cover the major genetic and geographic lineages revealed in a preliminary mitochondrial phylogenetic analysis based on cytochrome oxidase subunit 1 (COI) and 16S RNA (*rrn*L) gene fragments (Figure S1; Table S1). Most of the mitogenomes considered herein were obtained with 454 sequencing technology, using multiplexing by parallel-tagged libraries or by pooling untagged amplicons [20, 21]. Our main aims were (1) to derive a strongly supported phylogeny of the Metacrangonyctidae, sampling their full geographic distribution and (2) to estimate tree node ages using molecular dating techniques and paleogeographic calibration points. We aimed to test the hypothesis that species at opposite sides of the Atlantic had a vicariant origin, not a Mediterranean source followed by a secondary dispersal to the Caribbean.

Mitogenomic Phylogenies Solve Evolutionary Relationships within the Metacrangonyctidae

A Bayesian tree (Figure S2) was built using the full set of mitochondrial protein-coding genes (MPCGs) by implementing the

*Correspondence: jpons@imedea.uib-csic.es

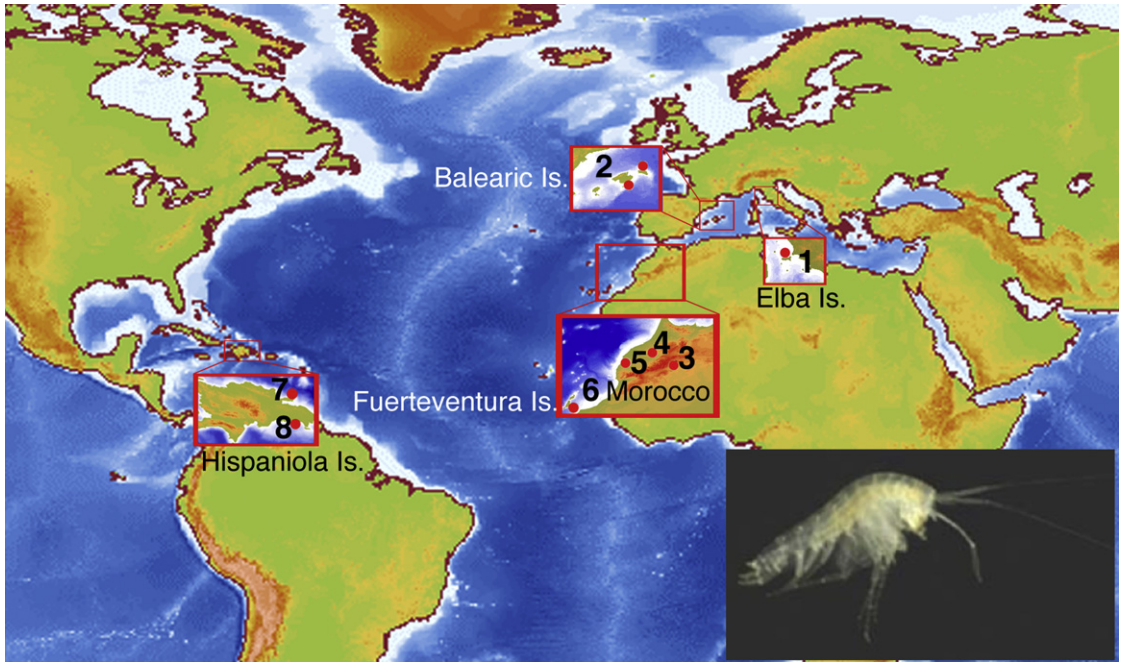

Figure 1. Metacrangonyctid Species Distribution

Map showing approximate geographic sampling locations of metacrangonyctid species for which whole mitochondrial genomes have been sequenced. See Table 1 and Table S1 for precise distribution of each taxon. 1, *Metacrangonyx ilvanus*; 2, *M. longipes*; 3, "M. notenboomi," *M. goulmimensis*, *M. longicaudus*, *M. spinicaudatus*, "M. paurosexualis," *M. panousei*; 4, *M. remyi*, "M. boveei"; 5, "L. stocki," "M. boutini boutini," "M. nicoleae tamri"; 6, *M. repens*; 7, *M. samanensis*; and 8, *M. dominicanus*. Inset shows *M. dominicanus* (photo by T.M. Iliffe). See also Figure S1.

best partition scheme and evolutionary models selected using the Bayesian Information Criterion (BIC; see Supplemental Experimental Procedures). Similar tree topologies were obtained using other partition schemes or the protein data set, but with discrepancies in the relationship among the taxa from Atlantic Morocco (they appeared as monophyletic in some analyses but paraphyletic in others) and in nodes relating the five insular species (Figure S2). The tree topology based on *SSU* sequences showed congruence with that obtained with MPCGs, but posterior probability values were low, particularly for basal nodes (Figure S2). The combined mitochondrial + *SSU* analyses supported paraphyly of the Atlantic Morocco lineages (Figure 2; Figure S2), but a Shimodaira-Hasegawa test showed that alternative topologies were not significantly different.

The tree recovered in the combined analysis (Figure 2) that we regard as our best phylogenetic hypothesis shows five strongly supported major clades within the family Metacrangonyctidae (here named A, B, C, D1, and D2). Each of these has a clearly delimited geographic projection, although B and C share the same overall area in Morocco. All tree topologies agreed on the assignment of an early divergence to "M. boveei" (tentative binomen) and *M. remyi* (clade A), which occur in the northern valleys and springs of the Western High Atlas in Morocco (Figures 1 and 2). Clade D appeared further subdivided into two strongly supported subclades: D1, present at both sides of the High Atlas in Morocco; and D2, embracing the five insular *Metacrangonyx* species from Mallorca-Menorca and Elba in the Mediterranean, Fuerteventura in the Canary Islands, and Hispaniola in the Caribbean. A Partition Bremer Support test taking each of the 13 MPCGs as a different partition suggested that the lack of resolution within the island subclade D2 arose from an absence of phylogenetic signal and not from incongruence among gene partitions (Figure S2). A further Bayesian analysis implementing a polytomy prior in Phycas (see Supplemental Experimental Procedures) also led to the rejection of a fully resolved tree in favor of a hard polytomy.

Several recent attempts to resolve the phylogeny and to explain the disjunct distributions of some atyid shrimp [9], remipedes [8], and cirolanid isopods [10] have been based only on partial mitochondrial and nuclear DNA sequences. Although mitogenome-based phylogenies represent a single locus and do not necessarily reflect the correct species tree, they have a considerably higher resolution power than partial (mitochondrial or nuclear) DNA sequences because of the large number of nucleotide positions considered and the high mutation rate exhibited by MPCGs. Our analysis of the phylogenetic relationships within the Metacrangonyctidae based on the 13 MPCGs with a partitioning by codon position plus the *SSU* nuclear marker produced an almost fully resolved tree except for the hard polytomy affecting insular clade D2.

Time Frame for Metacrangonyctid Diversification

Following the rejection of a strict molecular clock, we estimated node ages enforcing a relaxed molecular clock on the combined analysis topology assuming three independent substitution rates for each mitochondrial codon position. Two paleogeographic events were used to calibrate the tree. The divergence of the two lineages of *M. longipes* present on the Balearic archipelago was assumed to be associated with the complex geologic events that occurred in the Western Mediterranean from the Middle to the Late Miocene. Namely, the age for the complete separation of the Balearic Islands from other continental microplates detached from the Iberian

Table 1. Collection Sites and Mitochondrial Genome Sequence Information for Species Included in Analyses

Species	Locality	Mitogenome Length (bp)	*SSU* Length (bp)	Average Read Length (bp)	Coverage	Acc. N. Mitogenome	Acc. N. *SSU*
M. dominicanus Jaume and Christenson, 2001	Juan Dolio, S. Hispaniola (Dominican Rep.); well	14,543[d]	2,511	625	4.3×[a]	HE860499	HE967299
M. samanensis Jaume and Christenson, 2001	Samaná, N. Hispaniola (Dominican Rep.); well	14,067[f]	2,413	551	5.7×[a]	HE860505	HE967297
M. repens (Stock and Rondé-Broekhuizen, 1986)	Fuerteventura, Canary Is. (Spain); well	14,355	2,215	550	5.7×[a]	HE860495	HE967284
"M. nicolae tamri"	Aksri, NW Agadir (Morocco); spring near Talmat cave	13,517[e]	1,027+1268	411	145x[c]	HE860511	HE967292-3
"M. nicolae tamri"	Tamri, N. Agadir (Morocco); well	14,644	2,415	595	59×[b]	HE860504	HE967294
"M. boutini boutini"	Timzelite, Souss Massa NP, S. Agadir (Morocco); well	13,301[e]	2,357	433	107×[c]	HE860497	HE967295
M. panousei Balazuc and Ruffo, 1953	Agdz (Morocco); well	14,478[d]	2,295	453	80×[c]	HE860510	HE967289
M. goulmimensis Messouli, Boutin, and Coineau, 1991	Lamkedmyia Meleh Jorf, NW Erfoud (Morocco); well	14,507[d]	1,173	413	178×[c]	HE860500	HE967279
M. goulmimensis Messouli, Boutin, and Coineau, 1991	Ousroutou, E Rich, N. Errachidia (Morocco); well	14,602	2,179	454	100×[c]	HE860501	HE967278
M. goulmimensis Messouli, Boutin, and Coineau, 1991	Zouala maisson, S. Errachidia (Morocco); well	14,353	1,922	423	165×[c]	HE860502	HE967280
M. longicaudus Ruffo, 1954	Lamkedmyia Meleh Jorf, NW Erfoud (Morocco); well	14,712[d]	2,272	403	135×[c]	HE860509	HE967281
"M. notenboomi"	Maadid, NE Erfoud (Morocco); well	14,277[d]	2,275	420	168×[c]	HE860513	HE967298
"M. paurosexualis"	Souk Tben, Haouz Plain, Marrakech (Morocco); well	12,542[e]	2,370	424	94×[c]	HE860507	HE967291
M. spinicaudatus Karaman and Pesce, 1980	Souk Tben, Haouz Plain, Marrakech (Morocco); well	15,037	2,338	534	124×[b]	HE860506	HE967290
M. remyi Ruffo, 1953	Ijoukak, Western High Atlas (Morocco); spring at maison forestière	14,787[d]	2,246	454	281×[b]	HE860512	HE967287
"M. boveei"	L'Ourika valley, Western High Atlas (Morocco); well	15,012	2,299	511	100×[b]	HE860498	HE967288
"Longipodacrangonyx stocki'	Tafraut (Morocco); well	12,924[e]	337+1210	395	160×[c]	HE860496	HE967282-3
"Longipodacrangonyx stocki"	Arbaa-Sahe, SW Tiznit (Morocco); well	13,006[f]	N/A	431	103×[c]	HE860508	N/A
M. longipes Chevreux, 1909	Mallorca, Balearic Is. (Spain); Cala Varques Cave	14,113	2,200	NA	NA	AM944817	HE967285
M. longipes Chevreux, 1909	Menorca, Balearic Is. (Spain); Cala Figuera cave	14,117	2,087	437	87×[c]	HE861923	HE967286
M. ilvanus Stoch, 1997	Elba Island (Italy); well	14,770[d]	1,173	540	78×[b]	HE860503	HE967296
Pseudoniphargus daviui Jaume 1991	Cabrera, Balearic Is. (Spain); well	15,155	1,863	410	73×[b]	FR872383	HE967300
Bahadzia jaraguensis Jaume and Wagner 1988	Oviedo; S. Hispaniola (Dominican Rep.); cave	14,657	N/A	537	87×[b]	FR872382	N/A

See Table S1 for precise locations. Species names in quotes and not in italics denote taxa not formally described yet [17].
[a]Sanger method.
[b]Roche FLX/454 with tagging.
[c]Roche GS Junior with no tagging.
[d]Partial mitogenome due to A-T rich region was not completely sequenced.
[e]Partial mitogenome due to fragment comprising *rrn*L-*trn*S region was not completely sequenced.
[f]Partial mitogenome due to fragment including *rrn*S gene and A-T rich region was not completely sequenced.

rim (16 mya) and the Messinian Salinity Crisis (5.5 mya) were taken as the upper and lower bounds, respectively ([22, 23] and references therein). Furthermore, we assumed that the age of the node corresponding to the sister species *M. remyi* and "M. boveei," which dwell in neighboring valleys of the northern slopes of the Marrakech High Atlas in Morocco, cannot be younger than the uplift of this mountain range. According to [24], the Atlas domain remained submerged until the Middle Eocene (48.6–37.2 mya), the earliest uplift being dated as Late Eocene (37.2–33.9 mya), whereas the first significant folding extended through the entire Oligocene until the Early Miocene (25 mya). Thus, we propose to assign an age interval of 37.2–25.0 million years (my) to the last common ancestor of the two species.

Our chronogram (Figure 3) assigned an age of 96 my (with 95% higher posterior densities [HPDs] of 71–125 my) to the initial diversification that led to the contemporary metacrangonyctid lineages and suggests a mid-Cretaceous origin for the main clades of the family. Cross-validation showed that node ages estimated assuming the two foregoing paleogeographic events separately or by implementing different diversification models fell within the 95% HPDs of the estimations derived after considering the two calibration points altogether (Figure S3). An old lineage diversification at a remarkably small geographic scale took place in Morocco, where four of the five recognized monophyletic lineages concur, one of them resulting to be sister to the insular clade. Our estimated ages agree in general terms with those of Boutin [25] in the

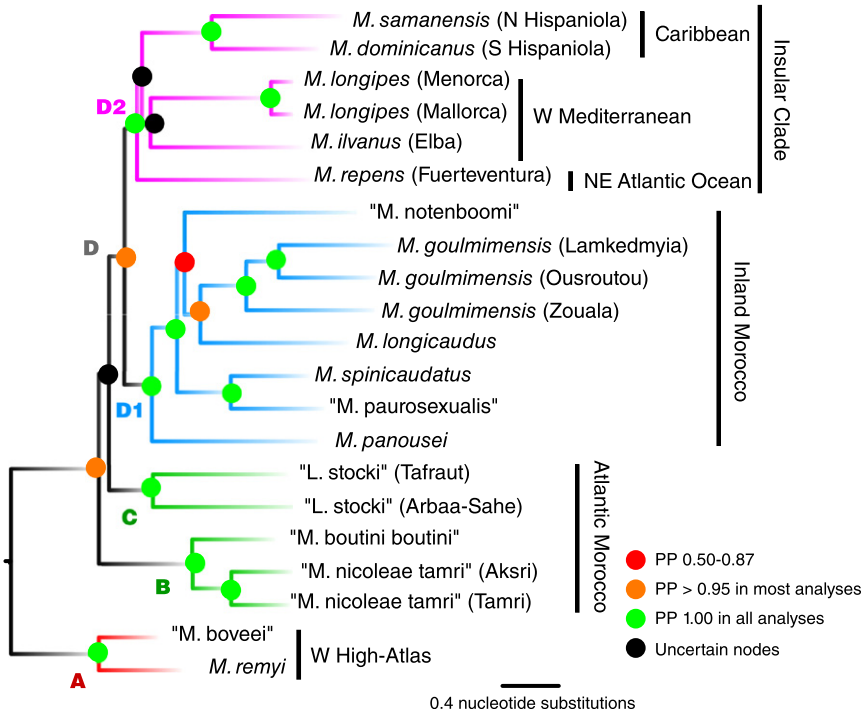

Figure 2. Mitogenomic + *SSU* Phylogenetic Tree of the Family Metacrangonyctidae

The topology was obtained from Bayesian analysis of combined mitochondrial protein-coding genes and 18S rRNA (*SSU*). The best partitioning scheme was selected based on Bayesian Information Criterion (GTR+I + Γ in first/second positions as different partitions, HKY+I + Γ for third mitochondrial codon positions and GTR+I + Γ for *SSU*) (see Table S2). Monophyly of the Metacrangonyctidae was supported with maximum posterior probability in all analyses (outgroups not shown). Dots of different colors at nodes summarize posterior probability support values obtained using different methods (details on topologies and support values for each analysis are shown in Figure S2).

assignment of a remarkably old age to the Metacrangonyctidae, with the differentiation of the major lineages in our phylogenetic reconstruction corresponding to the Cretaceous, c. 96–83 mya. This age range is coincident with the major Late Cretaceous Cenomano–Turonian transgression–regression cycle that affected most of the current Moroccan geography, and it was suggested to be the cause of individualization in continental groundwaters of some Moroccan lineages [25]. Our phylogeny shows that the insular species of *Metacrangonyx* (including the Caribbean and Mediterranean taxa) formed a strongly supported monophyletic group in all analyses (subclade D2), despite their extremely disjunct distribution. Remarkably, *M. repens* from Fuerteventura (Canary Islands) belongs to this insular clade and not to any of the geographically closer Moroccan clades. Two unresolved nodes account for the relationship between the Mediterranean insular species (Elba and Balearic Islands) and those of the Atlantic (Fuerteventura and Hispaniola). It has been suggested elsewhere that the difficulty in resolving phylogenetic relationships in subterranean amphipods might arise from the occurrence of sudden radiations associated with the synchronous colonization of groundwater by different populations of the same ancestor [2,26]. Our finding that the insular clade of *Metacrangonyx* diversified basally as a true polytomy is in agreement with the hypothesis of a simultaneous divergence ultimately leading to speciation in the isolated populations. The initial diversification of the insular clade is estimated to have occurred at 79 mya (95% HPDs 60–108 mya), a time frame compatible with the plate tectonics vicariance hypothesis if we consider the uncertainties associated with both the tectonic reconstruction of Tethys history and molecular clock estimations. Our estimated age for the divergence between the metacrangonyctids of Hispaniola and their Balearic sister group (77 mya; 95% HPDs 57–101 mya) lends additional support to this hypothesis. During that epoch, the Caribbean, the East Atlantic, and the portion of the Tethys Sea placed at the position of the Western Mediterranean formed a continuous seaway, and their shores and islands were placed much closer to each other than at present [27]. Note that Hispaniola Island, the Canary Islands and the entire Western Mediterranean basin had not yet formed at that time. The current Caribbean configuration is no older than the Late Eocene in age [28]; Fuerteventura, the oldest island of the Canary archipelago, dates back to 22 mya [29], whereas the entire Western Mediterranean basin formed at c. 20 mya [30]. However, there is compelling geologic evidence for the presence of drowned archipelagos and seamounts in the central East Atlantic since at least 60 mya [31–33]. These Paleo-Macaronesian islands were located much closer to the Western Mediterranean than today [33]. Ephemeral islands likely lasting a few million years each have been present in the Proto-Caribbean (volcanic islands, shallow banks and ridges) since the early Cretaceous [28]. Thus, the existence of these vanished archipelagos makes it likely that the ancestor of the insular lineage of *Metacrangonyx* was a shallow-water marine species that populated islands, shallow banks or strips of coast placed in this overall area, but not in the precise locations occupied by modern species.

Across the Metacrangonyctid mitochondrial protein-coding genes, we found an average long-term evolutionary rate of pairwise sequence divergence of 10.9% per million years. This is almost five times higher than the "standard" 2.3% of arthropod mitogenomes [34] and beetle MPCGs [35], or other rates estimated for the COI gene in marine decapods (1.4%–2.6% per million years) that have been applied frequently to other crustaceans [36]. If the "standard" 2.3% rate is used the estimated ages would be even older, thus not contradicting the main conclusion of an ancient vicariance. The only similar estimate to our knowledge is the 20% COI rate per million years obtained in the Hawaiian stygobiont decapod *Halocaridina rubra*, an accelerated evolution that has been related to the strong genetic structure and to the frequent occurrence of population bottlenecks in this species [37].

Other stygobiont crustacean groups such as remipedes and some ostracod, copepod, thermosbaenacean, and decapod lineages also display a presumed Tethyan distribution [38]. A clarification of their molecular phylogenies and timing of cladogenesis could shed light on the origin of their distribution

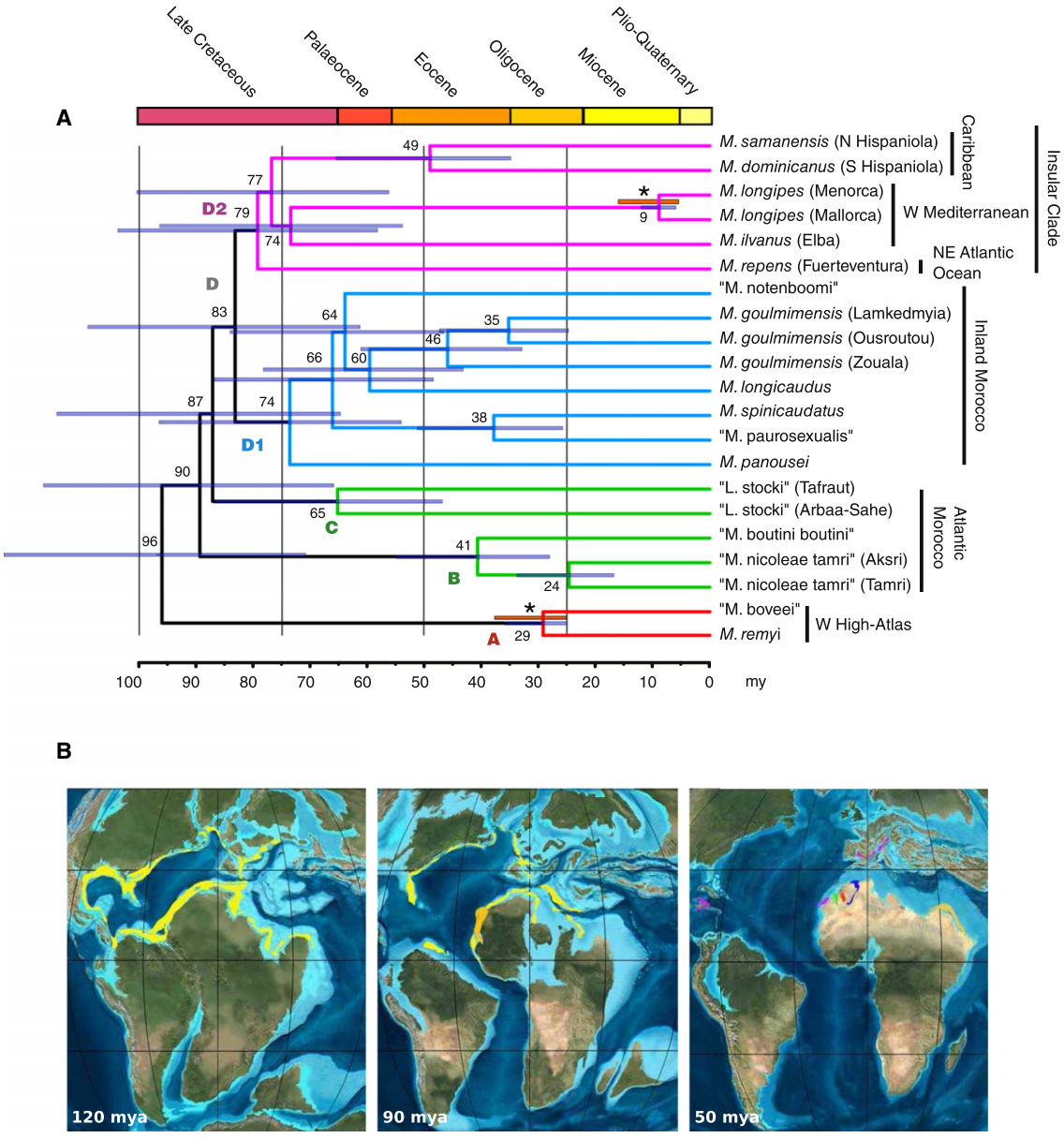

Figure 3. Time Frame for Diversification of the Metacrangonyctidae

(A) Shown are the divergence times for the Metacrangonyctidae estimated from Bayesian analysis of all mitochondrial protein-coding gene sequences based on two paleogeographic calibration points and a Yule diversification model (see main text and Supplemental Experimental Procedures). Mean values are indicated on nodes, whereas horizontal bars across nodes represent the 95% highest probability density intervals. Asterisks identify node constraints, with their respective age ranges in red, implemented as flat priors in the analysis. See also Figure S3 for ages estimated using single calibration points, strict clock, and Birth-Death models.

(B) Maps show global paleogeography at three different periods with corresponding putative metacrangonyctid distributions. Maps modified from Ron Blakey, NAU Geology (http://jan.ucc.nau.edu/~rcb7/globaltext2.html).

patterns in the context of the fragmentation of the Tethys Sea. Extensive mitochondrial data sets in combination with multiple nuclear loci obtained by next-generation DNA sequencing are a promising source of genetic information to unravel the process and timing of diversification of these stygobiont crustaceans.

Accession Numbers

Sequences obtained for this paper were deposited under EMBL accession numbers HE967026–HE967186 for COI, HE967187–HE967277 and HE970657–HE970663 for *rrn*L, FR872382-FR872383, HE860495-HE860513, and HE861923 for mitogenomes, and HE967278-HE967300 for *SSU*.

Supplemental Information

Supplemental Information includes three figures, two tables, and Supplemental Experimental Procedures and can be found with this article online at http://dx.doi.org/10.1016/j.cub.2012.09.012.

Acknowledgments

We are greatly indebted to C. Boutin, N. Coineau, M. Messouli, M. Yacoubi-Khebiza, and M. Boulanouar for support during fieldwork in Morocco, aid in species identification, and fruitful discussions. J.A. Ottenwalder and J.A. Alcover shared fieldwork in the Dominican Republic. J.M. Bichain and

A. Faille loaned Moroccan specimens collected in the frame of expedition Win-Timdouine 2008. We also thank F. Frati for hosting M.M.B.-R. at Department of Evolutionary Biology of the University of Siena. B. Emerson kindly advised and made comments on an earlier version of the manuscript. This work was supported by Spanish MCINN grant CGL2009-08256 and CSIC Intramural grant 200930I141, partially financed with EU FEDER funds. M.M.B.-R. benefited of a PhD Spanish FPI fellowship during the completion of this study.

Received: June 15, 2012
Revised: August 16, 2012
Accepted: September 5, 2012
Published online: October 11, 2012

References

1. Stock, J.H. (1993). Some remarkable distribution patterns in stygobiont Amphipoda. J. Nat. Hist. *27*, 807–819.
2. Notenboom, J. (1991). Marine regressions and the evolution of groundwater dwelling amphipods (Crustacea). J. Biogeogr. *18*, 437–454.
3. Väinölä, R., Witt, J.D.S., Grabowski, M., Bradbury, J.H., Jazdzewski, K., and Sket, B. (2008). Global diversity of amphipods (Amphipoda; Crustacea) in freshwater. Hydrobiologia *595*, 241–255.
4. Stock, J.H. (1977). The taxonomy and zoogeography of hadziid Amphipoda, with emphasis on the West Indian taxa. Stud. Fauna Curaçao Caribbean Isl. *55*, 1–130.
5. Stock, J.H. (1980). Regression mode evolution as exemplified by the genus *Pseudoniphargus* (Amphipoda). Bijdr. Dierk. *50*, 104–144.
6. Holsinger, J.R. (1986). Zoogeographic patterns of North American subterranean amphipod crustaceans. In Crustacean issues 4. Crustacean Biogeography, R.H. Gore and K.L. Heck, eds. (Rotterdam, Boston: A.A. Balkema), pp. 85–106.
7. Holsinger, J.R. (1988). Troglobites: The evolution of cave-dwelling organisms. Am. Sci. *76*, 146–153.
8. Neiber, M.T., Hartke, T.R., Stemme, T., Bergmann, A., Rust, J., Iliffe, T.M., and Koenemann, S. (2011). Global biodiversity and phylogenetic evaluation of Remipedia (crustacea). PLoS ONE *6*, e19627.
9. Page, T.J., Humphreys, W.F., and Hughes, J.M. (2008). Shrimps down under: Evolutionary relationships of subterranean crustaceans from Western Australia (Decapoda, Atyidae, *Stygiocaris*). PLoS One *3*, e1618.
10. Baratti, M., Filippelli, M., Nardi, F., and Messana, G. (2010). Molecular phylogenetic relationships among some stygobitic cirolanid species (Crustacea, Isopoda). Contrib. Zool. *79*, 57–67.
11. Holsinger, J.R. (1991). What can vicariance biogeographic models tell us about the distributional history of subterranean amphipods? Hydrobiologia *223*, 43–45.
12. Boxshall, G.A. (1989). Colonization of inland marine caves by misophrioid copepods. J. Zool. (Lond.) *219*, 521–526.
13. Sclater, J.G., Hellinger, S., and Tapscott, C. (1977). The paleobathymetry of the Atlantic Ocean from the Jurassic to the Present. J. Geol. *85*, 509–552.
14. Jones, E.J.W., Cande, S.C., and Spathopoulos, F. (1995). Evolution of a major oceanographic pathway: the equatorial Atlantic. J. Geol. Soc. London *90*, 199–213.
15. Boutin, C., and Messouli, M. (1988). *Longipodacrangonyx maroccanus* n. gen. n. sp., nouveau représentant du groupe *Metacrangonyx* dans les eaux souterraines du Maroc. Crustaceana *13* (suppl.), 256–271.
16. Messouli, M. (1988). Les Crustacés Amphipodes Souterrains du Groupe *Metacrangonyx*. Répartition, Systématique et Phylogénie. Ms Thesis. Université de Marrakech, Morocco, 234 pp.
17. Messouli, M. (1994). Evolution, Phylogénie et Biogéographie Historique des Metacrangonyctidae, Crustacés Amphipodes Stygobies du Nord de l'Afrique et des Régions Voisines. Ph.D Thesis. Université de Marrakech, Morocco, 312 pp.
18. Jaume, D., and Christenson, K. (2001). Amphi-Atlantic distribution of the subterranean amphipod family Metacrangonyctidae (Crustacea, Gammaridea). Contrib. Zool. *70*, 99–125.
19. Bauzà-Ribot, M.M., Jaume, D., Juan, C., and Pons, J. (2009). The complete mitochondrial genome of the subterranean crustacean *Metacrangonyx longipes* (Amphipoda): a unique gene order and extremely short control region. Mitochondrial DNA *20*, 88–99.
20. Meyer, M., Stenzel, U., Myles, S., Prüfer, K., and Hofreiter, M. (2007). Targeted high-throughput sequencing of tagged nucleic acid samples. Nucleic Acids Res. *35*, e97.
21. Timmermans, M.J.T.N., Dodsworth, S., Culverwell, C.L., Bocak, L., Ahrens, D., Littlewood, D.T.J., Pons, J., and Vogler, A.P. (2010). Why barcode? High-throughput multiplex sequencing of mitochondrial genomes for molecular systematics. Nucleic Acids Res. *38*, e197.
22. Bauzà-Ribot, M.M., Jaume, D., Fornós, J.J., Juan, C., and Pons, J. (2011). Islands beneath islands: phylogeography of a groundwater amphipod crustacean in the Balearic archipelago. BMC Evol. Biol. *11*, 221.
23. Bidegaray-Batista, L., and Arnedo, M.A. (2011). Gone with the plate: the opening of the Western Mediterranean basin drove the diversification of ground-dweller spiders. BMC Evol. Biol. *11*, 317.
24. Frizon de Lamotte, D., Zizi, M., Missenard, Y., Hafid, M., El Azzouzi, M., Maury, R.C., Charrière, A., Taki, Z., Benammi, M., and Michard, A. (2008). The Atlas System. In Continental Evolution: The Geology of Morocco, A. Michard, A. Chalouan, O. Saddiqi, and D. Frizon de Lamotte, eds. (Heidelberg: Springer), pp. 133–202.
25. Boutin, C. (1994). Phylogeny and biogeography of metacrangonyctid amphipods in North Africa. Hydrobiologia *287*, 49–64.
26. Lefébure, T., Douady, C.J., Malard, F., and Gibert, J. (2007). Testing dispersal and cryptic diversity in a widely distributed groundwater amphipod (*Niphargus rhenorhodanensis*). Mol. Phylogenet. Evol. *42*, 676–686.
27. Smith, A.G., Smith, D.G., and Funnell, B.M. (1994). Atlas of Mesozoic and Cenozoic Coastlines (Cambridge: Cambridge University Press), pp. 103.
28. Iturralde-Vinent, M.A. (2006). Meso-Cenozoic Caribbean paleogeography: Implications for the historical biogeography of the region. Int. Geol. Rev. *48*, 791–827.
29. Coello, J., Cantagrel, J.M., Hernan, F., Fuster, J.M., Ibarrola, E., Ancochea, E., Casquet, C., Jamond, C., Diaz De Teran, J.R., and Cendrero, A. (1992). Evolution of the eastern volcanic ridge of the Canary Islands based on new K-Ar data. J. Volcanol. Geotherm. Res. *53*, 251–274.
30. Alvarez, W. (1972). Rotation of the Corsica–Sardinia microplate. Nature *235*, 103–105.
31. Geldmacher, J., Hoernle, K., van den Bogaard, P., Zankl, G., and Garbe-Schönberg, D. (2001). Earlier history of the > 70-Ma-old Canary hotspot based on temporal and geochemical evolution of the Selvagems Archipelago and neighbouring seamounts in the eastern North Atlantic. J. Volcanol. Geotherm. Res. *111*, 55–87.
32. Geldmacher, J., Hoernle, K., van den Bogaard, P., Duggen, S., and Werner, R. (2005). New 40K/39Ar age and geochemical data from seamounts in the Canary and Madeira volcanic provinces: Support for the mantle plume hypothesis. Earth Planet. Sci. Lett. *237*, 85–101.
33. Fernández-Palacios, J.M., de Nascimento, L., Otto, R., Delgado, J.D., Garcıa-del-Rey, E., Arevalo, J.R., and Whittaker, R.J. (2011). A reconstruction of Palaeo-Macaronesia, with particular reference to the long-term biogeography of the Atlantic island laurel forests. J. Biogeogr. *38*, 226–246.
34. Brower, A.V.Z. (1994). Rapid morphological radiation and convergence among races of the butterfly *Heliconius erato* inferred from patterns of mitochondrial DNA evolution. Proc. Natl. Acad. Sci. USA *91*, 6491–6495.
35. Pons, J., Ribera, I., Bertranpetit, J., and Balke, M. (2010). Nucleotide substitution rates for the full set of mitochondrial protein-coding genes in Coleoptera. Mol. Phylogenet. Evol. *56*, 796–807.
36. Kornobis, E., Pálsson, S., Kristjánsson, B.K., and Svavarsson, J. (2010). Molecular evidence of the survival of subterranean amphipods (Arthropoda) during Ice Age underneath glaciers in Iceland. Mol. Ecol. *19*, 2516–2530.
37. Craft, J.D., Russ, A.D., Yamamoto, M.N., Iwai, T.Y., Jr., Hau, S., Kahiapo, J., Chong, C.T., Ziegler-Chong, S., Muir, C., Fujita, Y., et al. (2008). Islands under islands: The phylogeography and evolution of *Halocaridina rubra* Holthuis, 1963 (Crustacean: Decapoda: Atyidae) in the Hawaiian archipelago. Limnol. Oceanogr. *53*, 675–689.
38. Juan, C., Guzik, M.T., Jaume, D., and Cooper, S.J.B. (2010). Evolution in caves: Darwin's 'wrecks of ancient life' in the molecular era. Mol. Ecol. *19*, 3865–3880.

Current Biology, Volume *22*

Supplemental Information

Mitogenomic Phylogenetic Analysis Supports Continental-Scale Vicariance in Subterranean Thalassoid Crustaceans

Maria M. Bauzà-Ribot, Carlos Juan, Francesco Nardi, Pedro Oromí, Joan Pons, and Damià Jaume

Supplemental Inventory

1. Supplemental Figures and Tables

Figure S1, related to Figure 1

Figure S2, related to Figure 2

Figure S3, related to Figure 3

Table S1, related to Table 1

Table S2, related to Figure 2

2. Supplemental Experimental Procedures

3. Supplemental References

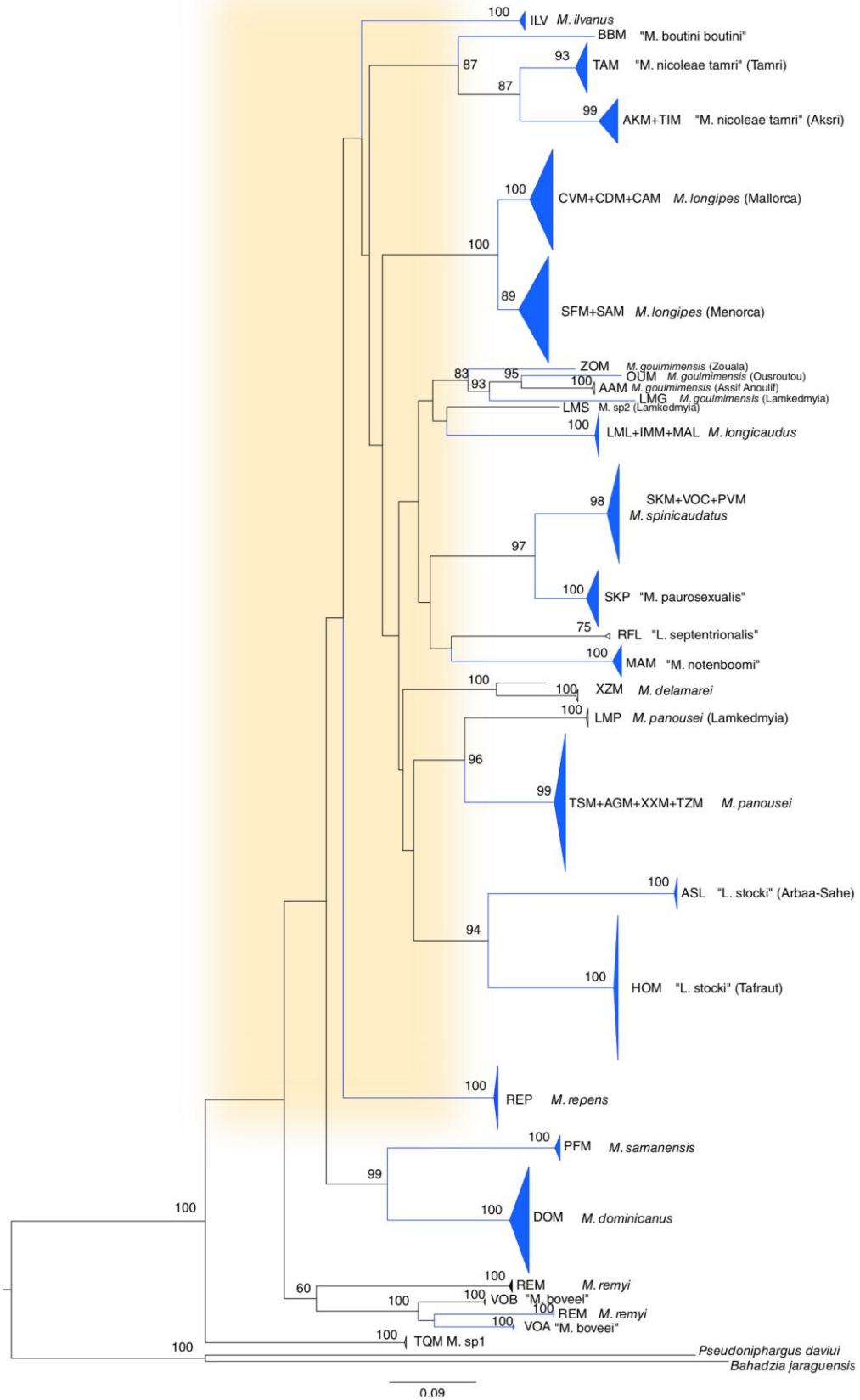

Figure S1. Metacrangonyctid Maximum Likelihood Tree of All 214 Specimens Based on Mitochondrial COI and rrnL (16S rRNA) Gene Fragments, Related to Figure 1

Lineages from which one representative species was selected for whole mitochondrial sequencing are shown in blue. Only bootstrap values ≥ 60 are shown on nodes. Note lack of support for many of basal nodes (colored background).

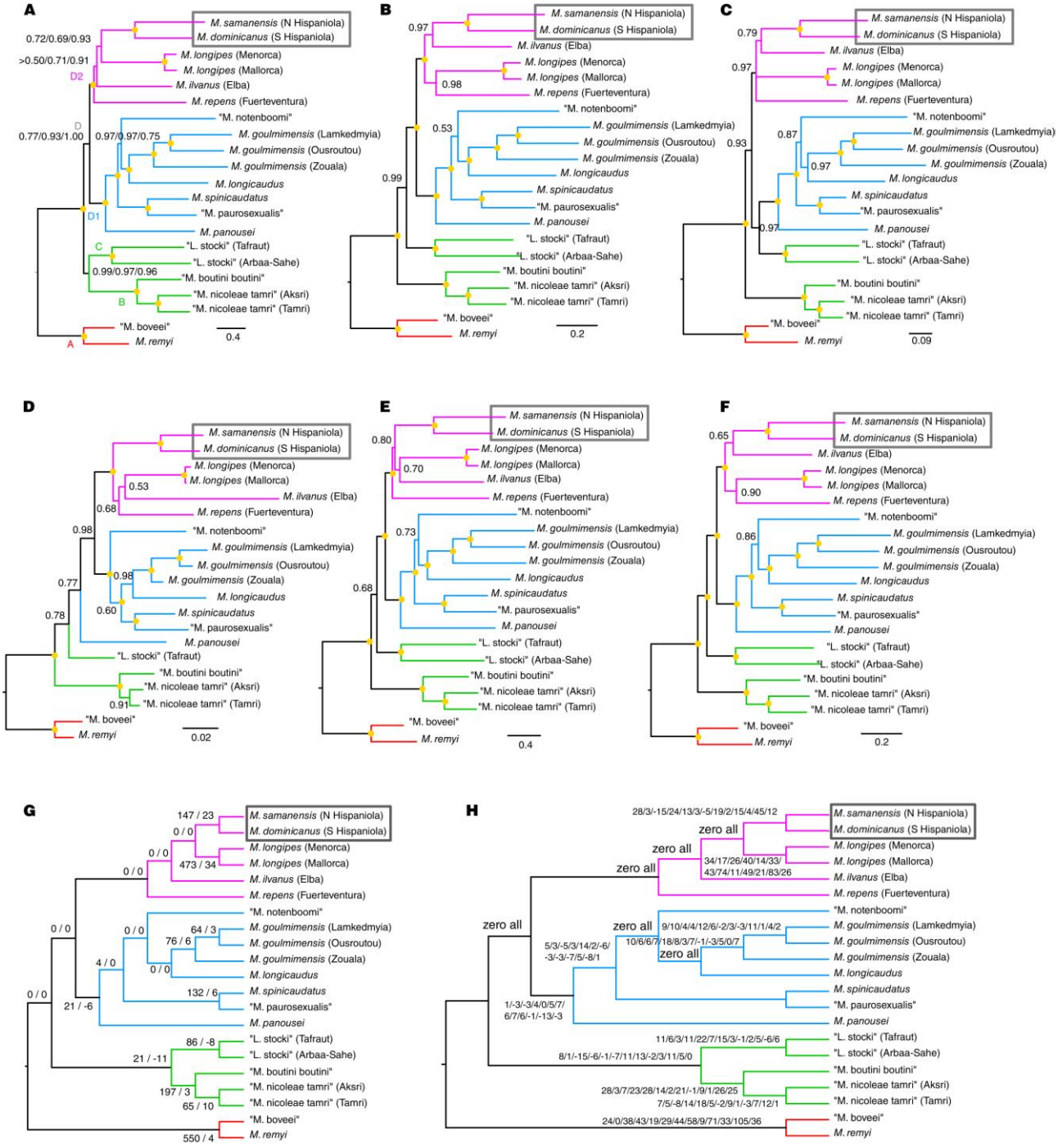
A
M. samanensis (N Hispaniola)
M. dominicanus (S Hispaniola)
0.72/0.69/0.93
>0.50/0.71/0.91
M. longipes (Menorca)
M. longipes (Mallorca)
D2
M. ilvanus (Elba)
M. repens (Fuerteventura)
D
0.77/0.93/1.00
0.97/0.97/0.75
"M. notenboomi"
M. goulmimensis (Lamkedmyia)
M. goulmimensis (Ousroutou)
M. goulmimensis (Zouala)
M. longicaudus
M. spinicaudatus
"M. paurosexualis"
D1
M. panousei
C
"L. stocki" (Tafraut)
"L. stocki" (Arbaa-Sahe)
0.99/0.97/0.96
"M. boutini boutini"
"M. nicoleae tamri" (Aksri)
B
"M. nicoleae tamri" (Tamri)
"M. boveei"
A
M. remyi
0.4
B
M. samanensis (N Hispaniola)
M. dominicanus (S Hispaniola)
0.97
M. ilvanus (Elba)
M. longipes (Menorca)
M. longipes (Mallorca)
0.98
M. repens (Fuerteventura)
"M. notenboomi"
0.53
M. goulmimensis (Lamkedmyia)
M. goulmimensis (Ousroutou)
M. goulmimensis (Zouala)
M. longicaudus
0.99
M. spinicaudatus
"M. paurosexualis"
M. panousei
"L. stocki" (Tafraut)
"L. stocki" (Arbaa-Sahe)
"M. boutini boutini"
"M. nicoleae tamri" (Aksri)
"M. nicoleae tamri" (Tamri)
"M. boveei"
M. remyi
0.2
C
M. samanensis (N Hispaniola)
M. dominicanus (S Hispaniola)
0.79
M. ilvanus (Elba)
0.97
M. longipes (Menorca)
M. longipes (Mallorca)
M. repens (Fuerteventura)
"M. notenboomi"
0.87
M. goulmimensis (Lamkedmyia)
M. goulmimensis (Ousroutou)
0.93
0.97
M. goulmimensis (Zouala)
M. longicaudus
M. spinicaudatus
"M. paurosexualis"
0.97
M. panousei
"L. stocki" (Tafraut)
"L. stocki" (Arbaa-Sahe)
"M. boutini boutini"
"M. nicoleae tamri" (Aksri)
"M. nicoleae tamri" (Tamri)
"M. boveei"
M. remyi
0.09
D
M. samanensis (N Hispaniola)
M. dominicanus (S Hispaniola)
M. longipes (Menorca)
M. longipes (Mallorca)
0.53
M. ilvanus (Elba)
0.68
M. repens (Fuerteventura)
0.98
"M. notenboomi"
M. goulmimensis (Lamkedmyia)
M. goulmimensis (Ousroutou)
0.77
0.98
M. goulmimensis (Zouala)
M. longicaudus
0.60
0.78
M. spinicaudatus
"M. paurosexualis"
M. panousei
"L. stocki" (Tafraut)
"M. boutini boutini"
"M. nicoleae tamri" (Aksri)
0.91
"M. nicoleae tamri" (Tamri)
"M. boveei"
M. remyi
0.02
E
M. samanensis (N Hispaniola)
M. dominicanus (S Hispaniola)
0.80
M. longipes (Menorca)
0.70
M. longipes (Mallorca)
M. ilvanus (Elba)
M. repens (Fuerteventura)
"M. notenboomi"
0.73
M. goulmimensis (Lamkedmyia)
M. goulmimensis (Ousroutou)
M. goulmimensis (Zouala)
M. longicaudus
0.68
M. spinicaudatus
"M. paurosexualis"
M. panousei
"L. stocki" (Tafraut)
"L. stocki" (Arbaa-Sahe)
"M. boutini boutini"
"M. nicoleae tamri" (Aksri)
"M. nicoleae tamri" (Tamri)
"M. boveei"
M. remyi
0.4
F
M. samanensis (N Hispaniola)
M. dominicanus (S Hispaniola)
0.65
M. ilvanus (Elba)
M. longipes (Menorca)
0.90
M. longipes (Mallorca)
M. repens (Fuerteventura)
"M. notenboomi"
0.86
M. goulmimensis (Lamkedmyia)
M. goulmimensis (Ousroutou)
M. goulmimensis (Zouala)
M. longicaudus
M. spinicaudatus
"M. paurosexualis"
M. panousei
"L. stocki" (Tafraut)
"L. stocki" (Arbaa-Sahe)
"M. boutini boutini"
"M. nicoleae tamri" (Aksri)
"M. nicoleae tamri" (Tamri)
"M. boveei"
M. remyi
0.2
G
M. samanensis (N Hispaniola)
M. dominicanus (S Hispaniola)
147 / 23
0 / 0
M. longipes (Menorca)
0 / 0
M. longipes (Mallorca)
473 / 34
0 / 0
M. ilvanus (Elba)
M. repens (Fuerteventura)
"M. notenboomi"
0 / 0
0 / 0
64 / 3
M. goulmimensis (Lamkedmyia)
76 / 6
M. goulmimensis (Ousroutou)
4 / 0
M. goulmimensis (Zouala)
0 / 0
M. longicaudus
0 / 0
132 / 6
M. spinicaudatus
21 / -6
"M. paurosexualis"
M. panousei
86 / -8
"L. stocki" (Tafraut)
21 / -11
"L. stocki" (Arbaa-Sahe)
"M. boutini boutini"
197 / 3
"M. nicoleae tamri" (Aksri)
65 / 10
"M. nicoleae tamri" (Tamri)
"M. boveei"
550 / 4
M. remyi
H
28/3/-15/24/13/3/-5/19/2/15/4/45/12
M. samanensis (N Hispaniola)
M. dominicanus (S Hispaniola)
zero all
zero all
M. longipes (Menorca)
zero all
34/17/26/40/14/33/
43/74/11/49/21/83/26
M. longipes (Mallorca)
M. ilvanus (Elba)
M. repens (Fuerteventura)
"M. notenboomi"
zero all
9/10/4/4/12/6/-2/3/-3/11/1/4/2
M. goulmimensis (Lamkedmyia)
zero all
10/6/6/7/18/8/3/7/-1/-3/5/0/7
M. goulmimensis (Ousroutou)
5/3/-5/3/14/2/-6/
-3/-3/-7/5/-8/1
zero all
M. goulmimensis (Zouala)
M. longicaudus
M. spinicaudatus
"M. paurosexualis"
1/-3/-3/4/0/5/7/
6/7/6/-1/-13/-3
M. panousei
11/6/3/11/22/7/15/3/-1/2/5/-6/6
"L. stocki" (Tafraut)
8/1/-15/-6/-1/-7/11/13/-2/3/11/5/0
"L. stocki" (Arbaa-Sahe)
"M. boutini boutini"
28/3/7/23/28/14/2/21/-1/9/1/26/25
"M. nicoleae tamri" (Aksri)
7/5/-8/14/18/5/-2/9/1/-3/7/12/1
"M. nicoleae tamri" (Tamri)
24/0/38/43/19/29/44/58/9/71/33/105/36
"M. boveei"
M. remyi

Figure S2. Phylogenetic Trees Obtained using Different Data Partitioning and Evolutionary Models, Related to Figure 2

Numbers on nodes of trees A-F denote Bayesian posterior probabilities lower than 1, whereas nodes with a yellow dot have posterior probability = 1. Caribbean species are highlighted within a box. A) Tree obtained using either mitocondrial protein coding genes (MPCGs) as a single partition (first number), two partitions (first and second codon positions as one and third positions as another partition, second number) and each codon position as a different partition (third number). B) MPCGs implementing the Goldman Yang codon model. C) MPCGs as amino acid sequences. D) SSU alone. E) Combined MPCGs partitioned by codon position + SSU as a fourth partition. F) MPCGs implementing the Goldman Yang codon model + SSU. G) Partition Bremer Support analysis of MPCGs vs. SSU datasets. First number refers to parsimony steps for MPCGs and second for SSU. Negative numbers indicate topology conflict of the SSU partition with the topology obtained using MPCGs. H) Partition Bremer Support analysis of the 13 MPCGs. Numbers refer to parsimony steps for the genes as separate partitions in the following order: *atp6, atp8, cob, cox1, cox2, cox3, nad1, nad2, nad3, nad4, nad4L, nad5* and *nad6.*

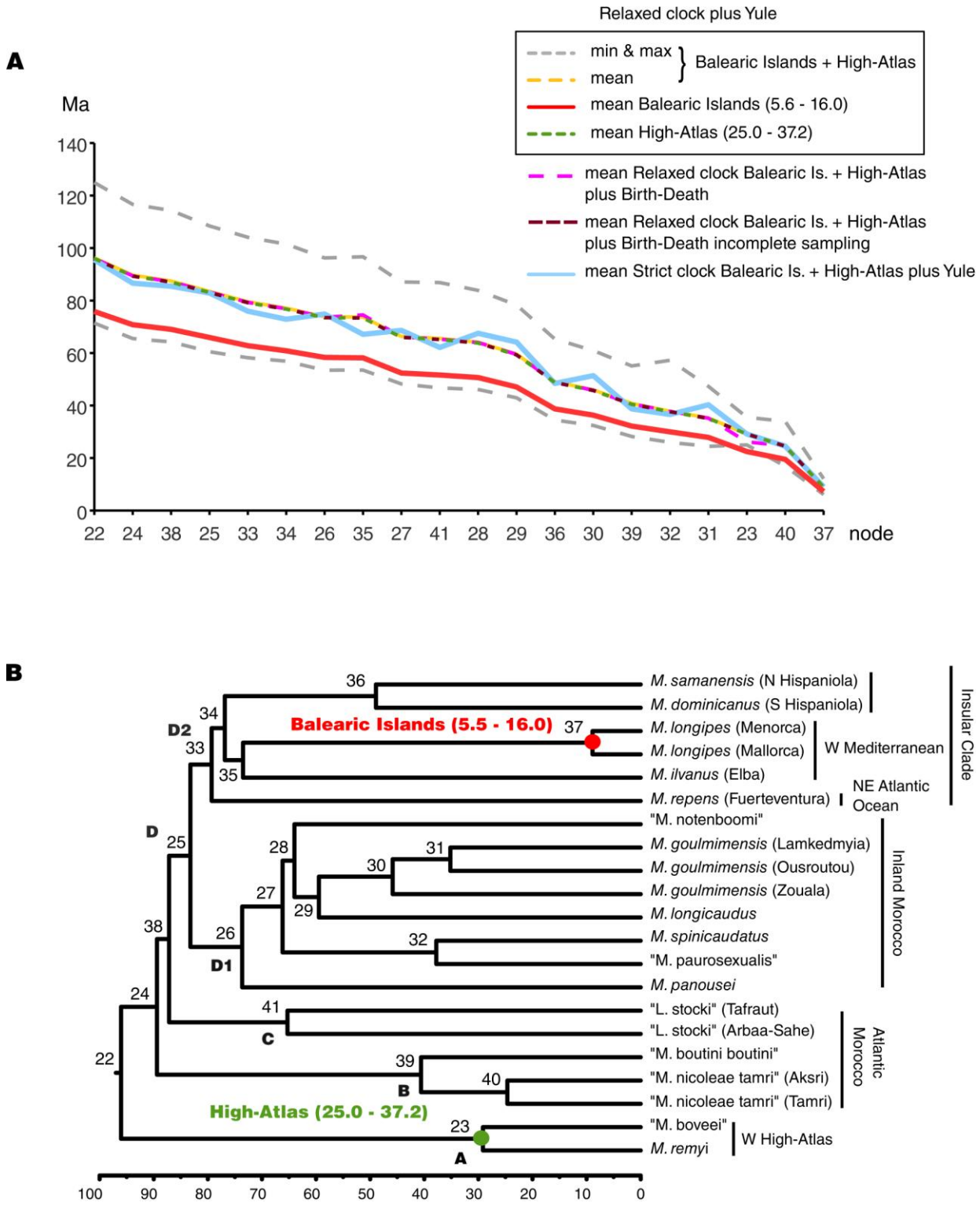
A
Relaxed clock plus Yule
min & max
mean
Balearic Islands + High-Atlas
mean Balearic Islands (5.6 - 16.0)
mean High-Atlas (25.0 - 37.2)
mean Relaxed clock Balearic Is. + High-Atlas plus Birth-Death
mean Relaxed clock Balearic Is. + High-Atlas plus Birth-Death incomplete sampling
mean Strict clock Balearic Is. + High-Atlas plus Yule
Ma
140
120
100
80
60
40
20
0
22 24 38 25 33 34 26 35 27 41 28 29 36 30 39 32 31 23 40 37
node
B
36
34
D2
33
35
Balearic Islands (5.5 - 16.0)
37
M. samanensis (N Hispaniola)
M. dominicanus (S Hispaniola)
M. longipes (Menorca)
M. longipes (Mallorca)
M. ilvanus (Elba)
M. repens (Fuerteventura)
W Mediterranean
NE Atlantic Ocean
Insular Clade
D
25
28
31
30
27
29
38
26
D1
32
"M. notenboomi"
M. goulmimensis (Lamkedmyia)
M. goulmimensis (Ousroutou)
M. goulmimensis (Zouala)
M. longicaudus
M. spinicaudatus
"M. paurosexualis"
M. panousei
Inland Morocco
24
41
C
"L. stocki" (Tafraut)
"L. stocki" (Arbaa-Sahe)
22
39
B
40
"M. boutini boutini"
"M. nicoleae tamri" (Aksri)
"M. nicoleae tamri" (Tamri)
Atlantic Morocco
High-Atlas (25.0 - 37.2)
23
A
"M. boveei"
M. remyi
W High-Atlas
100 90 80 70 60 50 40 30 20 10 0

Figure S3. Estimation of Node Ages, Related to Figure 3

A) Comparison of node age estimates assuming one or two palaeogeographical events under relaxed or strict clocks, and Yule or Birth-Death diversification models. The split of the two M. longipes lineages of the Balearic archipelago was calibrated with a flat prior of 16 to 5.5 Ma, and the divergence of M. remyi and “M. boveei” at the High-Atlas with a flat prior of 37.2 -25 Ma. Minimum and maximum ages within the 95% HPDs (grey), and mean values (yellow) assuming both palaeogeographical age constrains and a relaxed clock and Yule are indicated by dotted lines. Mean values for single calibration points for Balearic Islands and High-Atlas constraints are shown in red and green, respectively. Mean ages obtained assuming a strict clock and both constrains are indicated in blue and for Birth-Death and incomplete Birth-Death in pink and brown, respectively.

B) Ultrametric tree showing corresponding node numbers, and node age constrains.

Table S1. *Metracrangonyx* and *Longipodacrangonyx* Species included in the Preliminary Phylogeny, Related to Table 1

Species	Code	Location	Geographic coordinates	COI	*rrn*L
"Longipodacrangonyx septentrionalis"	RFL	Sidi Abdellah, Taza (Morocco); well	N32.55000º W7.83333º	2	0
"Longipodacrangonyx stocki"	ASL	Arbaa-Sahe, SW Tiznit (Morocco); well	*N29º36.568' W9º55.187'	6	6
	HOM	Tafraut (Morocco); well	*29R 502729 / 3288806	24	5
M. s. spinicaudatus Karaman & Pesce, 1980	SKM	Souk Tben, Haouz Plain, Marrakech (Morocco); well	*N31º42.698' W8º04.257'	12	9
	PVM	Puit de la Porte Verde, Haouz Plain, Marrakech (Morocco); well	*N31º39.594' W8º01.243'	3	3
	VOC	L'Ourika valley, Western High Atlas (Morocco); well	*N31º22.551' W7º46.779'	1	1
"M. paurosexualis"	SKP	Souk Tben, Haouz Plain, Marrakech (Morocco); well	*N31º42.698' W8º04.257'	9	3
"M. boveei"	VOA	L'Ourika valley, Western High Atlas (Morocco); well	*N31º17.302' W7º 42.632'	2	2
	VOB	L'Ourika valley, Western High Atlas (Morocco); well	*N31º18.560' W07º44.545'	2	1
M. remyi Ruffo, 1953	REM	Ijoukak, Western High Atlas (Morocco); spring at maison forestière (REM01-03)	*N30º59.895' W8º08.847'	3	3
		Agoundiss river; near Ijoukak (Morocco); spring (REM04-05)	N/A	2	1
"M. nicoleae tamri"	TAM	Tamri, N Agadir (Morocco); well	*N30º42.791' W9º46.761'	9	9
	AKM	Aksri, NW Agadir (Morocco); spring near Talmat cave	N30°36.852' W9°28.129'	4	3
	TIM	Tizgni N'Chorfa, NW Agadir (Morocco); Tifrit spring	N30°39.096' W9°21.637'	2	2
		Tizgni N'Chorfa, NW Agadir (Morocco); Win-Timdouine cave	N30º40'50" W9º20'42"	2	2
"M. boutinin boutini"	BBM	Timzelite, Souss Massa NP, S Agadir (Morocco); well	*29R 423825 / 3300524	1	1
M. dominicanus Jaume & Christenson, 2001	DOM	Juan Dolio (Dominican Rep.); well (DOM01-06)	* N18º26.083' W69º25.860'	6	1
		Juan Dolio (Dominican Rep.); well (DOM07-DOM10)	*N18º26.076' W69º25.776'	4	3
		Juan Dolio (Dominican Rep.); well (DOM11)	*N18º26.407' W69º25.551'	1	1
		Juan Dolio (Dominican Rep.); well (DOM12)	*N18º26.434' W69º25.689'	1	0
		Juan Dolio (Dominican Rep.); well (DOM13-18)	N/A	6	0
M. samanensis Jaume & Christenson, 2001	PFM	Playa Frontón, Samaná Peninsula (Dominican Rep.); well	*N19º17.799' W69º9.118'	5	1
M. repens Stock & Rondé-Broekhuizen,1986	REP	Betancuria, Fuerteventura, Canary Is. (Spain); well beside church (REP01)	*28R 592366 / 3144662	1	1
		Betancuria, Fuerteventura, Canary Is. (Spain); well (REP03-08; REP12-13)	*28R 591749 / 3142183	8	2
		Barranco del Cigarrón, Llanos de la Concepción, Fuerteventura, Canary Is. (Spain); well (REP14-15)	*28R 590606 / 3151572	2	0
M. longipes Chevreux, 1909	SFM	Sant Lluís, Menorca, Balearic Is. (Spain); Ses Figueres cave	*31S 607475 / 4408145	13	4
	SAM	Ciutadella, Menorca, Balearic Is. (Spain); S'Aigo cave	*31S 4424877 / 571259	5	3
	CVM	Porto Cristo, Mallorca, Balearic Is. (Spain); Cala Varques C cave	# 31S 4372450 / 525550	8	3
	CDM	Ses Salines, Mallorca, Balearic Is. (Spain); Dracs cave	*31S 4353625 / 512830	5	3
	CAM	Sant Llorenç, Mallorca, Balearic Is. (Spain); S'Abisament cave	*N39º34.570'E03º22.233	4	3
M. ilvanus Stoch, 1997	ILV	Elba Island (Italy); well	# 32T 610505 / 4737245	4	4
M. panousei Balazuc & Ruffo, 1953	XXM	Avant Agdz (Morocco); well	N30.66950º W6.33145º	5	5
	AGM	Agdz (Morocco); well	N30.691570º W6.447630º	3	3
	TZM	Tamzoulin Draa, SE of Agdz (Morocco); well	N30.508410º W6.102380º	1	1

	TSM	4 km before Tasla on road coming from Agdz (Morocco); well	*N30º34.613' W6º42.502'	15	4
	LMP	Lamkedmyia Meleh Jorfn NW Erfoud (Morocco); well	N31.50063º W4.39498º	4	0
M. goulmimensis Messouli, Boutin & Coineau, 1991	AAM	Assif Anoulif, W Rich, NW of Errachidia (Morocco); hyporheic	N32.26544º W4.809340º	3	3
	OUM	Ousroutou, E Rich, N Errachidia (Morocco); well	N32.258770º W4.533420º	1	1
	LMG	Lamkedmyia Meleh Jorf; NW Erfoud (Morocco); well	N31.50063º W4.39498º	1	1
	ZOM	Zouala maisson, S Errachidia (Morocco); well	N31.789380º W4.247950º	1	1
M. longicaudus Ruffo, 1954	LML	Lamkedmyia Meleh Jorf; NW Erfoud (Morocco); well	N31.50063º W4.39498º	5	5
	IMM	Imiter, E Boulmane Dadès (Morocco); well	N31.377701º W5.796114º	2	2
	MAL	Maadid, NE Erfoud (Morocco); well	N31.48178º W4.21749º	1	1
M. delamarei Messouli, Boutin & Coineau, 1991	XZM	Ouarzazat (Morocco); well	N30.90687° W6.91112°	4	4
"M. notenboomi"	MAM	Maadid, NE Erfoud (Morocco); well	N31.48178^{0} W4.21749º	6	4
Metacrangonyx sp1	TQM	Tiqqi, NW Agadir (Morocco); Doussoulile cave	N30°44.529' W9°19.803'	3	2
Metacrangonyx sp2	LMS	Lamkedmyia Meleh Jorf; NW Erfoud (Morocco); well	N31.50063º W4.39498º	1	1

Code of sampling locations, geographical coordinates, and number of sequenced individuals for two mitochondrial genes (COI and *rrn*L) are indicated. Geographic coordinates with Datum WGS84 (*), and with Datum ED50 (#) were taken directly on spot with GPS recorder, and those with no datum indicated were derived from Google Maps images. Species names not in italics and with inverted commas refer to taxa not formally described yet (see main text).

Table S2. Likelihood (Ln) Values for Each Partition Scheme Tested Calculated Using Garli v. 2.0, Related to Figure 2

Garli-analysis	Ln	free parameters (K)	BIC
single partition	-149781.809	9	299647.484
1st + 2nd vs 3rd codon sites	-145801.879	16	291752.854
1st vs 2nd vs 3rd codon sites	-144816.827	26	289875.935
by gene (13)	-148918.591	124	298992.673
Goldman & Yang codon model	-147746.836	67	296118.010

Best evolutionary model for each partition was estimated in jModeltest v0.1.1, and best partitioning scheme was selected based on Bayesian Information Criterion (BIC). Analyses included two outgroup taxa. BIC= 2Ln + K ln n (n = Number of characters 11142 bp).

Supplemental Experimental Procedures

Taxon Sampling and Preliminary Selection of Taxa

We sampled 214 specimens assigned to 17 species of *Metacrangonyx* and to two species of *Longipodacrangonyx* from freshwater wells and anchialine caves spanning almost the entire known geographic range of the family (we failed to collect specimens from the Middle East). Several Moroccan taxa included in our analyses that are not formally described yet are quoted with a tentative Latinized binomen with inverted commas and not in italics to identify this feature. Sampling locations with their geographic coordinates and the numbers of individuals studied per site are listed in Table S1. Two mitochondrial genes (COI and *rrn*L) from this set of taxa were sequenced initially and analyzed to obtain a preliminary maximum likelihood phylogenetic tree for the family. Based on the results (Figure S1), 19 *Metacrangonyx* and two *Longipodacrangonyx* taxa were identified as representatives of the major lineages within the family (in several cases individuals of the same morphospecies showed unexpectedly large genetic divergences, suggesting the occurrence of cryptic species) and were selected for sequencing of the entire mitogenome and the nearly complete small nuclear ribosomal subunit (*SSU*) (Table 1 in main text).

Amplification of Mitochondrial and Nuclear Markers

Long-range polymerase chain reaction (PCR) primers were designed on available COI and *rrn*L sequences to amplify the entire genomes of *Metacrangonyx* and *Longipodacrangonyx* plus two outgroups as two overlapping long amplicons (see list below). Alternatively, the mitogenomes of four species were amplified as a single long fragment with primers targeting the *rrn*L and *rrn*S genes. Long-range PCR amplifications were performed using 1–2 μL aliquots of the genomic DNA (~100 ng) as template and Herculase TM II Fusion DNA polymerase (Agilent, Santa Clara, CA, USA) according to the manufacturer's specifications.

Nuclear *SSU* ribosomal sequences were amplified using primers designed by [1] and newly designed ones for *Metacrangonyx* (5′–3′): 18s-F123 (CGGCTCATTAAATCAGTCTTGG); 18s-R2605 (GTAGTAGCGACGGGCGGTG); 18s-F651 (AGAACCTACTGAAGGGCAAG); 18s-F1228 (GAGTAAATCAGAGTGCTCAAAG); and 18s-F1553 (TGCCAACCATCAATCCGC). PCR products were sequenced using traditional Sanger cycle sequencing and internal primers (see above).

Long PCR Primer list.

Species	Code	Fragment	Primer	Sequence
M. dominicanus	DOM	*cox*1-*rrn*L	MetDom_*cox*1F4	GAGAATAGTTGAGAGGGGGGTAGGG
			MetDom_16s_R3	TGAAAACTGGAATGAAGGGTCTAACAA
		*rrn*L-*cox*1	MetDom_16s_F3	TTGTTATACCCTTCATTCCAGTTTTCA
			MetDom_*cox*1_R	CCTACCCCCCTCTCAACTATTCTCC
M. samanensis	PFM	*cox*1-*rrn*L	Sam_*cox*1_F1	CTGGGCTAGGATAGTGGGTACTGCTA
			Sam_16s_R6	AAATAAAAAGGAAAGGATTAAGTTACTCTAGGG
		*rrn*L-*cox*1	Sam_16s_F7	TATCCAGAACTATTACGCTGTTATCCCTAGAG
			Sam_*cox*1_R4	GGTCCATTTTTATCCCAGTAACTCG
M. repens	REP	*cox*1-*rrn*L	Repens_*cox*1_F8	GGTCATAGTGGTTGTTCTGTAGATTTGG
			Repens_16s_R12	AATGGGATGTAAAAGTTACTCTAGGGATA
		*nad*1-*cox*1	Repens_nad1_F5	CCCAGATATAAATCCACACCCCCTTC
			Repens_*cox*1_R9	CAACCAGTTCCTACTCCACTCTCCAC
M. ilvanus	ILV	*cox*1-*rrn*L	Ilv_*cox*1_F5	GAGGTATGGTAGAAAGAGGAGTTGGTACAGG
			Ilv_16s_R2	GGATAACAGCGTAATAATTTTGGATAGCCC
		*rrn*L-*cox*1	Ilv_16s_F2	GGCTATCCAAAATTATTACGCTGTTATCCC
			Ilv_*cox*1_R2	CAGTCCATCCTGTACCAACTCCTCTTTCTACC
"M. nicoleae tamri"	TAM	*cox*1-*rrn*L	Tam_*cox*1_F1	TAGTATAGTGGGGACGGCAATAAGGG
			Tam_16s_R2	AGTTACTCTAGGGATAACAGCGTAATAATTTTGG
		*rrn*L-*cox*1	Tam_16s_F1	AAGGTCTAACCAAAATTATTACGCTGTTATCCC
			Tam_*cox*1_R1	TGTTCATCCTGTCCCTACTCCTCTCTCCAC

Species	Code	Fragment	Primer	Sequence
M. spinicaudatus	SKM	*cox*1-*rrn*L	SpinSK_*cox*1_F2	ACTGATAAGAAGAATAGTAGAAAGAGGCGTAGG
			SpinSK_16s_R3	TTGGAAACTGGAATGAAAGGTTAAACAAT
		*rrn*L-*cox*1	SpinSK_16s_F1	GGTCTATCCAAAATTATCACGCTGTTATCCC
			SpinSK_*cox*1_R2	CAACCTGTACCTACGCCTCTTTCTACTATTCTTC
“M. boveei”	VOB	*cox*1-*rrn*L	Bov6_*cox*_F1	GAGAATAGTAGAAAGAGGGGTAGGGACGGG
			Bov6_16s_R1	ATTGGGGACTAGAATGAAAGGTTTTACAACTTATG
		*rrn*L-*cox*1	Bov6_16s_F3	ATTCATAAGTTGTAAAACCTTTCATTCTAGTCCCC
			Bov6_*cox*1_R2	CCGTCCCTACCCCTCTTTCTACTATTCTCC
M. remyi	REM	*cox*1-*rrn*L	Rem_*cox*1_F3	GACTGTTTACCCTCCTTTATCCAGAGTTATTGC
			Rem_16s_R1	CGATGTTGAATTAAAATATCCCTGTAGAGTAGAAAC
		*rrn*L-*cox*1	Rem_16sF3	TATAAGCCGTGGGACCCTTCATTCTAGTC
			Rem_*cox*1R3	TCCAACCAGTTCCTACCCCTCTTTCTACTATT
M. longicaudus	LML	*cox*1-*rrn*L	IMLM_*cox*1_F2	ATAAGAAGAATAGTAGAGAGAGGAGTAGGGACTGG
			IMLM_16s_R1	TAATTGGGAACTGGAATGAAGGGTTGAAC
		*rrn*L-*cox*1	IMLM_16s_F1	GATCTATCCAAAATTATCGTGCTGTTATCCC
			IMLM_*cox*1_R2	TGAAAAAATAGCCAAATCCACCGAAGC
M. panousei	AGM	*cox*1-*rrn*L	AGTS_*cox*1_F1	GCCAGAATGGTAGGCACTGCTATAAGAG
			AGTS_16s_R1	ATCTGAGGTTTGAATAACTTTGATTGGGG
		*rrn*L-*cox*1	AGTS_16s_F1	CCTATCCAAAATTATTACGCTGTTATCCCTAG
			AGTS_*cox*1_R4	TCAACCTGTTCCTACTCCTCTTTCAACTATTC
M. goulmimensis	OUM	*cox*1-*rrn*L	OUM_*cox*1_F1	ATTGGAGGGTTTGGTAATTGACTATTGCC
			OUM_16s_R1	TTAATTGGAGACTGGAATGAAAGGTTGAAC
		*rrn*L-*cox*1	OUM_16s_F2	TTGTTCAACCTTTCATTCCAGTCTCC
			OUM_*cox*1_R1	GCAATAGTCAATTACCAAACCCTCC
	LMG	*cox*1-*rrn*L	L10_*cox*1F3	GTAGAGAGAGGTGTAGGGACGGGG
			L10_16sR1	ATTGGAAACTGGAATGAAGGGTTG
		*rrn*L-*cox*1	L10_16sF2	AAAAATTGTTCAACCCTTCATTCC
			L10_*cox*1R3	CACCCCGTCCCTACACCTCTCTC
	ZOM	*cox*1-*rrn*L	ZOM_*cox*1F3	AAGAAGAATAGTAGAAAGGGGAGCCG
			ZOM_16sR1	TAGGGATAACAGCGTAATAATTTTGGATAG
		*rrn*L-*cox*1	ZOM_16sF1	TATCCAAAATTATTACGCTGTTATCCC
			ZOM_*cox*1R1	CGGCTCCCCTTTCTACTATTCTTC
“Longipodacrangonyx	HOM	12s-*rrn*L	Uni_Meta_12sF	TATTGTAACTAATCTAATTTTAARTATATCTGCACCT
			Uni_Meta_16sR	ATTTTTTACATGATTTGAGTTCAGACCG
	ASL	12s-*rrn*L	Uni_Meta_12sF	TATTGTAACTAATCTAATTTTAARTATATCTGCACCT
			Uni_Meta_16sR	ATTTTTTACATGATTTGAGTTCAGACCG
“M. paurosexualis”	SKP	12s-*rrn*L	Uni_Meta_12sF	TATTGTAACTAATCTAATTTTAARTATATCTGCACCT
			Uni_Meta_16sR	ATTTTTTACATGATTTGAGTTCAGACCG
“M. boutini boutini”	BBM	12s-*rrn*L	Uni_Meta_12sF	TATTGTAACTAATCTAATTTTAARTATATCTGCACCT
			Uni_Meta_16sR	ATTTTTTACATGATTTGAGTTCAGACCG
“M. nicoleae tamri”	AKM	12s-*rrn*L	Uni_Meta_12sF	TATTGTAACTAATCTAATTTTAARTATATCTGCACCT
			Uni_Meta_16sR	ATTTTTTACATGATTTGAGTTCAGACCG
M. longipes	SFM	*cox*1-nad1	Met_nd1F1	CAGTATTAAATCCTGACACAAGCTCTGAACCTCTCTC
			Met_16s_R1	TGAAAAATAGAAAGTATAGCCTGCCC
		*rrn*L-*cox*1	Met_16sF2	CTATCCAAAATTATTACGCTGTTATCCC
			Met_*cox*1R2	GAAGAAGTCAGTTACCGAACCCTCC
“M. notenboomi”	MAM	*cox*1-*rrn*L	MAM_*cox*1F3	ATGGTAGAAAGAGGGGTTGGTACAGGATG
			MAM_16sR1	ATTGTTTTTTAATTGAGAACTGGAATGAAAGG
		*rrn*L-*cox*1	MAM_16sF1	CCTATCCAAAATTATTACGCTGTTATCC
			MAM_*cox*1R5	ACCAACCCCTCTTTCTACCATTCTAC
Bahadzia jaraguensis	BAH	*cox*1-*rrn*L	Bah_*cox*1_F3	GGACAGTTTATCCTCCATTAGCAGCAGC
			Bah_16s_R3	GGAGAGATCATATCTATAAAATTGATTGCGACC
		*rrn*L-*cox*1	Bah_16s_F1	GAGGTCGCAATCAATTTTATAGATATGATCTCTCC
			Bah_*cox*1_R2	GCTGTAATGAAGACTGACCAAGCAAATAAAGG
Pseudoniphargus daviui	PSN	*cox*1-*rrn*L	Pni_*cox*1_F2	CAGACATAGCCTTCCCTCGCATAAATAAC
			Pni_16s_R1	AAATACTATAATAAAATAAAGTGACGATAAGACCCTATA
		*rrn*L-*cox*1	Pni_16s_F1	ATCTTATGCTCATCCATCAATGTAAAACTCAC
			Pni_*cox*1_R1	GTTATTTATGCGAGGGAAGGCTATGTCTG

Full Genome Sequencing Using Sanger and Next-generation Methods

Initial sequencing (*M. repens, M. dominicanus, M. samanensis*) was conducted using a Shearing/Shotgun Sequencing approach with an average of 5 × coverage [2]. The remaining genomes were produced by pyrosequencing of libraries using either the Roche FLX/454 or GS Junior systems, giving a total number of 200,000 to 100,000 reads, respectively, and a minimum coverage of 59 × (Table 1 in the main text). Sequences were matched to genomes using either specific tagged libraries or species-specific "bait" sequences (see main text for references).

Mitogenome Analyses, Assembly, and Annotation

Part of the control region or a small sequence fragment placed between *rrn*L and *rrn*S genes could not be recovered in 10 out of the 23 mitogenomes because of technical difficulties (Table 1, main text), while the rest were fully resolved. The refined complete or nearly complete (see above) sequence of each genome was obtained through a CodonCode Aligner (v. 3.7; CodonCode Corporation, Denham, MA, USA) assembly of high-quality sequences (score > 400). Indels and homopolymeric regions were inspected by eye and a decision on the length of homopolymeric tracts was based on: a) observed frequency of reads with different number of bases, and b) constraints imposed by the reading frame at protein-coding genes or conserved secondary structures in tRNAs. Details of mean sequence lengths, numbers of reads, coverage and accession numbers for the mitochondrial sequence of each species are indicated in Table 1 (main text). Protein-coding genes, ribosomal RNAs and tRNAs were annotated with the DOGMA webserver (http://mailman.uk.freebsd.org/pipermail/ukfreebsd/2002-September/007710.html). tRNA secondary structures were further checked using tRNAscan-SE v. 1.21 [3] and edited by eye following the secondary structure model of [4]. Mitogenome size ranged between 14 and 15 kb, with an average A + T content in protein-coding genes of 72.73% (range 67.53–75.94%). Gene order in all metacrangonyctid species was identical to that for *Metacrangonyx longipes*, which in turn differs from the Pancrustacean ancestral pattern. The two outgroup taxa *P. daviui* and *B. jaraguensis* also showed a different gene order with respect to both *Metacrangonyx* and the Pancrustacean pattern.

Phylogenetic Analyses

Phylogenetic analyses of mitochondrial genomes were based on protein-coding genes only. Nucleotide sequences of individual mitochondrial protein-coding genes (MPCGs), excluding terminal stop codons, were retroaligned based on the corresponding protein translation [5, 6] and concatenated as needed. We used the test of Xia and Lemey [7] to check for substitution saturation in the mitochondrial sequences. For the MPCGs' first, second and third codon positions, the I_{ss} values (index of substitution saturation) were 0.4644, 0.1609 and 0.6692, respectively. The critical I_{ssc} values (critical index of substitution saturation) for the number of taxa and sequence lengths in our dataset were 0.8107–0.8197. Thus, there was no substitution saturation at second positions and moderate-to-low saturation at the first and third positions, but the I_{ss} values obtained in all cases were significantly lower than the critical I_{ssc} values.

Nuclear *SSU* ribosomal sequences were aligned using MAFFT 4.0 considering RNA secondary structures [8] and analyzed alone or added as an additional partition to mitogenome data in some analyses. Ambiguously aligned blocks were removed using

Gblocks v. 0.91b with relaxed parameters [9]. We explored the best partition scheme for the mitochondrial dataset comparing the following: a) a single partition; b) first and second codon positions into a single partition and third as another set; c) by codon position; d) by gene; and e) by codon model [10]. Likelihood values for each partition scheme were calculated using Garli v. 2.0 [11] and the best partitioning scheme was selected based on Bayesian Information Criterion (BIC). The best nucleotide substitution model for each partition was estimated with the Perl script MrAIC [12] based on BIC (Table S3). MrBayes v. 3.1.2 was used to perform phylogenetic Bayesian analyses [13], taking advantage of a largely parallel Beagle-based implementation on a Tesla 2050 graphic card [14]. Each Bayesian search consisted of two independent runs of five million generations with three heated and one cold chain each, starting from default prior values and random trees. All parameters were unlinked and rates were allowed to vary freely over partitions. Burn-in and parameter/run convergence were assessed using Tracer v. 1.5 [15], aiming at an effective sample size greater than 200. After discarding the initial 10% of trees as burn-in, trees from the stationary phase of both runs were combined to obtain a majority rule tree and *a posteriori* node probabilities [13]. Analyses performed using the codon model of Goldman and Yang [10] were run for 20–30 million generations to ensure sufficient effective sample size after convergence. A burn-in value of 75% was applied in this case. Additional Bayesian analyses without any *a priori* partition scheme were also implemented in PhyloBayes v. 3.3 [16] using the CAT model (classifies sites into CATegories), grouping nucleotide or amino acid positions in K categories with similar specific rates and compositions. The global exchange rates were inferred from the data as recommended for datasets larger than 1,000 positions [16]. Three independent runs were performed and considered to converge when the maximum split frequency was lower than 0.1 and effective sample size was greater than 100 [16]. The lack of resolution observed at the base of subclade D2 was further considered. Partition Bremer Support analyses were performed with Treerot v 3.0 [17] in PAUP v. 4b10 [18], performing 200 random replicates to assess the presence of conflicting signals across genes. Preliminary maximum likelihood trees were obtained in RAxML 7.0.4 [19] and alternative tree topologies were compared using the Shimodaira–Hasegawa test [20]. Phycas v. 1.2.0 (http://www.phycas.org) [21] was used to test for the occurrence of a true polytomy: i.e., the outcome of a biologically true concurrent diversification and not of an artifact arising from a conflicting signal in the data. Priors of $e1$ or $e2$ were tested in this analysis, implying that a fully resolved tree needs to have a likelihood of one or two units higher to be favored over a tree with a polytomy. Two independent runs of 50,000 cycles (corresponding to about five million generations in MrBayes) with one cold and one heated chain were sampled every five cycles.

Estimation of Divergence Time

The combined MPCGs + *SSU* topology was used for branch-length optimization in BEAST v. 1.7.2 [22] using the mitochondrial dataset only, given the difficulty of modeling deletions and insertions in the *SSU* alignments. The analyses were performed using the preferred evolutionary models (GTR+I + Γ for first/second and HKY+I + Γ in third codon positions) and assuming either a birth–death with or without incomplete sampling or a Yule diversification model. Default priors were used to estimate the birth–death parameters: mean growth rate and relative death rate were drawn from uniform distributions with zero and infinite bounds. In this analysis, we also assumed three independent substitution rates implemented as three clocks with independent rates for the first, second and third codon positions to account for the different saturation levels at each position. Analyses were run for 100 million generations, sampling every 1,000 generations. The output was analyzed using Tracer v. 1.5 after discarding the first 10 million generations, ensuring that all

parameters had converged showing effective sample size values greater than 200. For tree calibration, we used two major paleogeographic events affecting the diversification of two *Metacrangonyx* lineages as flat priors: one occurring in the Balearic Islands (16.0–5.5 mya) and another in the High Atlas mountains (37.2–25.0 mya, see main text). The performance of a strict molecular clock versus a relaxed clock was compared based on Bayes Factors (BFs) in Tracer v. 1.5 showing that the relaxed clock was preferred (BF = 167.93, $p < 0.001$). We implemented an uncorrelated lognormal distribution of rates as recommended in [22], as it has been shown to outperform other methods [23]. A cross-validation procedure [24] was finally performed in which the relaxed molecular clock was alternatively calibrated with the age of one of the two nodes to check for consistency of the obtained age estimates. Similar age estimations were obtained using a birth–death model—either considering missing species or not—or a Yule diversification model and using the alternative monophyletic or paraphyletic tree topologies for clades B and C.

Sequences were deposited under EMBL accession numbers HE967026–HE967186 for COI and HE967187–HE967277 and HE970657–HE970663 for *rrn*L. Sequences for *M. longipes* had accession numbers FR846024–FR846060 and FR729731–FR729892 for *rrn*L and COI, respectively. Accession numbers for the *SSU* and mitogenome sequences are listed in Table 1 (main text).

Supplemental References

1. Englisch, U., Coleman, C.O., and Wägele, J.W. (2003). First observations on the phylogeny of the families Gammaridae, Crangonyctidae, Melitidae, Niphargidae, Megaluropidae and Oedicerotidae (Amphipoda, Crustacea), using small subunit rDNA gene sequences. J. Nat. Hist. *37*, 2461–2486.
2. Carapelli, A., Comandi, S., Convey, P., Nardi, F., and Frati, F. (2008). The complete mitochondrial genome of the Antarctic springtail *Cryptopygus antarcticus* (Hexapoda, Collembola). BMC Genomics *9*, 315.
3. Schattner, P., Brooks, A.N., and Lowe, T.M. (2005). The tRNAscan-SE, snoscan and snoGPS web servers for the detection of tRNAs and snoRNAs. Nucleic Acids Res. *33*, W686-689.
4. Kumazawa ,Y., and Nishida, M. (1993) Sequence evolution of mitochondrial tRNA genes and deep-branch animal phylogenetics. J. Mol. Evol. *37*, 380-398.
5. Abascal, F., Zardoya, R., and Telford, M.J. (2010). TranslatorX, multiple alignment of nucleotide sequences guided by amino acid translations. Nucleic Acids Res. *38*, W7-13.
6. Katoh, K., and Toh, H. (2008). Recent developments in the MAFFT multiple sequence alignment program. Brief Bioinform. *9*, 276-285.
7. Xia, X., and Lemey, P. (2009). Assessing substitution saturation with DAMBE. In The Phylogenetic Handbook: A Practical Approach to DNA and Protein Phylogeny, 2nd edition, P. Lemey, M. Salemi and A.M. Vandamme, eds. (Cambridge: University Press), pp. 615-630.
8. Katoh, K., and Toh, H. (2008). Improved accuracy of multiple ncRNA alignment by incorporating structural information into a MAFFT-based framework. BMC Bioinformatics *9*, 212.
9. Talavera, G., and Castresana, J. (2007). Improvement of phylogenies after removing divergent and ambiguously aligned blocks from protein sequence alignments. Syst. Bio. *56*, 564-577.
10. Goldman, N., and Yang, Z. (1994). A codon-based model of nucleotide substitution for protein-coding DNA sequences. Mol. Biol. Evol. *11*, 725-736

11. Zwickl, D. (2006). Genetic algorithm approaches for the phylogenetic analysis of large biological sequence datasets under the maximum likelihood criterion. PhD thesis, University of Texas at Austin, TX.

12. Nylander, J.A., Ronquist, F., Huelsenbeck, J.P., and Nieves-Aldrey J.L. (2004). Bayesian phylogenetic analysis of combined data. Syst. Biol. *53*, 47-67.

13. Huelsenbeck, J.P., and Ronquist, F. (2001). MrBAYES Bayesian inference of phylogenetic trees. Bioinformatics *17*, 754-755.

14. Suchard, M.A., and Rambaut, A. (2009). Many-core algorithms for statistical phylogenetics. Bioinformatics *25*, 1370-1376.

15. Rambaut, A., and Drummond, A.J. (2007). Tracer v. 1.4. Available from, <http, //beastbioedacuk/Tracer/>.

16. Lartillot, N., Lepage, T., and Blanquart, S. (2009). PhyloBayes 3, a Bayesian software package for phylogenetic reconstruction and molecular dating. Bioinformatics *25*, 2286-2288.

17. Sorenson, M.D., and Franzosa, E.A. (2007). TreeRot, version 3 Boston University, Boston, MA.

18. Swofford, D.L. (2002). PAUP 4.0 b10, Phylogenetic analysis using parsimony, (Sunderland: Sinauer Associates).

19. Stamatakis, A. (2006). RAxML-VI-HPC: Maximum Likelihood-based Phylogenetic Analyses with Thousands of Taxa and Mixed Models. Bioinformatics *22*, 2688-2690.

20. Shimodaira, H., and Hasegawa, M. (1999). Multiple comparisons of log-likelihoods with applications to phylogenetic inference. Mol. Biol. Evol. *16*, 1114–1116.

21. Lewis, P.O., Holder, M.T., and Holsinger, K.E. (2005). Polytomies and Bayesian phylogenetic inference. Syst. Biol. *54*, 241-253.

22. Drummond, A.J., and Rambaut, A. (2007). BEAST, Bayesian evolutionary analysis by sampling trees. BMC Evol. Biol. *7*, 214.

23. Lepage, T., Bryant, D., and Lartillot, N. (2007). A general comparison of relaxed molecular clock models. Mol. Biol. Evol. *24*, 2669-2680.

24. Near, T.J., Meylan, P.A., and Shaffer, H.B. (2005). Assessing concordance of fossil calibration points in molecular clock studies, an example using turtles. Am. Nat. *165*, 137-46.